

2004

Effects of the Antarctic ozone hole on southern hemisphere midlatitudes

Bhuvana KrishnaSharma
San Jose State University

Follow this and additional works at: https://scholarworks.sjsu.edu/etd_theses

Recommended Citation

KrishnaSharma, Bhuvana, "Effects of the Antarctic ozone hole on southern hemisphere midlatitudes" (2004). *Master's Theses*. 2617.
DOI: <https://doi.org/10.31979/etd.jxxb-86q3>
https://scholarworks.sjsu.edu/etd_theses/2617

This Thesis is brought to you for free and open access by the Master's Theses and Graduate Research at SJSU ScholarWorks. It has been accepted for inclusion in Master's Theses by an authorized administrator of SJSU ScholarWorks. For more information, please contact scholarworks@sjsu.edu.

EFFECTS OF THE ANTARCTIC OZONE HOLE ON SOUTHERN
HEMISPHERE MIDLATITUDES

A Thesis

Presented to

The Faculty of the Department of Meteorology

San José State University

In Partial Fulfillment

of the Requirements for the Degree

Master of Science

by

Bhuvana KrishnaSharma

August 2004

UMI Number: 1424488

INFORMATION TO USERS

The quality of this reproduction is dependent upon the quality of the copy submitted. Broken or indistinct print, colored or poor quality illustrations and photographs, print bleed-through, substandard margins, and improper alignment can adversely affect reproduction.

In the unlikely event that the author did not send a complete manuscript and there are missing pages, these will be noted. Also, if unauthorized copyright material had to be removed, a note will indicate the deletion.



UMI Microform 1424488

Copyright 2005 by ProQuest Information and Learning Company.

All rights reserved. This microform edition is protected against unauthorized copying under Title 17, United States Code.

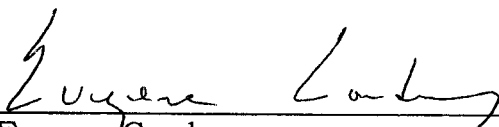
ProQuest Information and Learning Company
300 North Zeeb Road
P.O. Box 1346
Ann Arbor, MI 48106-1346

© 2004

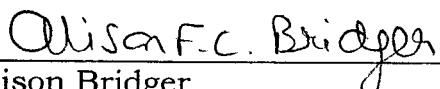
Bhuvana KrishnaSharma

ALL RIGHTS RESERVED

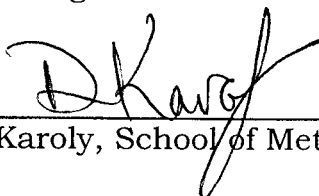
APPROVED FOR THE DEPARTMENT OF METEOROLOGY



Dr. Eugene Cordero

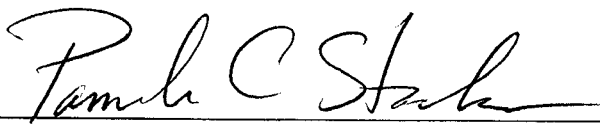


Dr. Alison Bridger



Dr. David Karoly, School of Meteorology, University of Oklahoma

APPROVED FOR THE UNIVERSITY



ABSTRACT

EFFECTS OF THE ANTARCTIC OZONE HOLE ON SOUTHERN HEMISPHERE MIDLATITUDES.

by Bhuvana KrishnaSharma

A three-dimensional chemical transport model incorporating chemistry using parameterized production-loss rates, and driven by assimilated winds, is used to isolate the effects of the Antarctic ozone hole (AOH) on southern midlatitudes. Simulations with and without polar stratospheric cloud (PSC) chemistry are performed for the years 1997-2000. It is found that, averaged over a period between 1997-2000, a ~3.7% decline in the midlatitudes column ozone can be attributed to the PSC-initiated polar ozone losses. The springtime midlatitude ozone loss resulting from the polar decline is greatest (-4.9%) in 2000 and smallest (-2.5%) in 1999. The observed difference in the year-to-year AOH midlatitude contribution depends upon the interannual variations in the strength of extratropical planetary wave numbers 1 and 2. While wave 1 is more important in polar-midlatitude transport during September-October, wave 2 exhibits a greater significance in November-December.

ACKNOWLEDGMENTS

I would like to express my gratitude to all the people who have contributed to the completion of my thesis work. First, to Dr. Eugene Cordero, my research advisor, who introduced to the field of middle atmospheric dynamics and gave me an opportunity to work on a global phenomenon-the Antarctic ozone hole. I am thankful to him for all the suggestions that he offered from me time to time during my research. I also appreciate his help in my learning IDL that has been used for the graphical analysis involved in this work.

I would also like to thank my other thesis committee members, Dr. Alison Bridger and Dr. David Karoly for their valuable comments. Mike Voss helped in running the chemical transport model used in this study; I would like to thank him for this and for all the computing support he gave me during my research.

My sincere appreciation to all the faculty members, staff, and students of Meteorology Department San José State University, for providing the friendly environment I experienced during my thesis work.

TABLE OF CONTENTS

Abstract.....	iv
Acknowledgements.....	v
List of Tables.....	vii
List of Figures.....	ix
1. INTRODUCTION.....	1
a. Ozone.....	2
b. Stratospheric ozone: Chemistry and Dynamics.....	3
c. Natural Ozone Variability	5
d. Anthropogenic Ozone Variability.....	6
e. Antarctic Ozone Hole.....	7
f. Impact of the AOH on Midlatitudes.....	10
g. Interannual variability in Midlatitudes Ozone	12
h. Project Goals.....	14
2. MODEL AND DATASETS	15
a. Description	15
b. Data Sources: Input and Analysis	17
c. Model Performance.....	18
d. Model Simulations	20
3. RESULTS AND DISCUSSION.....	21
a. Impact on midlatitudes	21
b. Interannual Variability	26
4. CONCLUSIONS	32
REFERENCES	35

LIST OF TABLES

Table 1 - Difference in total ozone between PSC and No PSC run, in DU, for the polar regions (averaged between 90°S-60°S), the midlatitudes (averaged between 60°S and 30°S) and for the different midlatitudes regions (60°S-50°S, 50°S-40°S, 40°S-30°S), for the years 1997-2000.	43
Table 2 - Difference in total ozone between PSC and No PSC run, in DU, for the midlatitudes (averaged between 60°S and 30°S) (MAF) for individual months between September and December during 1997-2000.	44
Table 3 - Average and maximum deviation from NO-PSC chemistry in the modeled midlatitude (60°S- 30°S) total ozone (in %), for the years 1997-2000.....	45
Table 4 - Comparison of the modeled maximum midlatitude (60°S-30°S) total ozone deviation with the TOMS present /pre-ozone hole maximum midlatitude (60°S-30°S) total ozone deviation for the for September-December period of 1997-2000.	46
Table 5 - Comparison of the correlation coefficient factors between the midlatitude AOH factor (MAF)/Polar ozone losses and normalized intensity of the 100hPa geopotential height wave 1 and 2 at 60° S for the years 1997-2000.	47

LIST OF FIGURES

Figure 1 - Schematic of zonally averaged transport in the stratosphere. The lines with arrows show the zonal-mean circulation, and the double-ended arrows indicate rapid adiabatic mixing. The shaded regions (at the edge of the polar vortex and the edge of the tropics) indicate the limits of this rapid mixing (Adapted from http://www.meteorology.monash.edu.au/info/techup1.pdf).	48
Figure 2- Annual mean, zonal mean cross section of ozone mixing ratio (ppmv) derived from MLS satellite data spanning 1991-96. Contour interval is 1 ppmv (Adapted from Atkinson 1997).	49
Figure 3- Climatological total ozone seasonal cycle, constructed using potential vorticity coordinates (expressed in equivalent latitude). Contours are in DU. The bracketed x's denote the statistical vortex edge region in the lower stratosphere (Adapted from Randel and Wu 1995).	50
Figure 4- Daily total ozone time series from the Australian ground-based monitoring stations for the period from July 1995 to June 1996. Missing values have been replaced by the time series mean (Adapted from Atkinson 1997).	51
Figure 5- Measured total ozone above the Halley Bay station in Antarctica, where each point represents the average total ozone for the month of October (Adapted from http://www.atm.ch.cam.ac.uk/tour/tour_images/total_ozone.gif)...52	52
Figure 6- Annual variation of Southern hemisphere polar stratospheric temperature, showing wintertime temperatures facilitating PSC type I formation that starts polar ozone losses (Adapted from NCEP-CPC Statistical and Climatological Analyses system at http://code916.gsfc.nasa.gov).	53
Figure 7- Percentage deviations in midlatitude total ozone between 1980 and 2000 for both Northern and Southern hemispheres (Adapted from Scientific Assessment of ozone Depletion: WMO 2002).	54
Figure 8- Schematic representation summarizing the dual roles of the extratropical planetary waves following Newman et al. 2002 and Li et al. 2002.	55
Figure 9- Total column ozone (in DU) on October 15 and November 18 of 1997 for the southern hemisphere, with left panels taken from observations (TOMS) and right panels from the CTM.	56

Figure 10- Vertical profile of ozone at 55°S on September 16, 1997 obtained from the CTM compared with the ozonesonde profile at the same location.	57
Figure 11- Production and Loss Coefficients of NASA 2-D model with and without PSC modifications at 12km on September 15.	58
Figure 12- Difference in total ozone, in DU, between the two runs for the midlatitudes region (60°S-30°S), isolating the AOH contribution to midlatitudes, for the year 1997-2000. The plots are valid for the period September-December.....	59
Figure 13 - Time series of the total ozone deviation in the midlatitudes (60°S-30°S) between the CTM PSC and NO PSC runs for 1997-2000.	60
Figure 14- Total ozone at midlatitudes (60°S-30°S) from TOMS, comparing the pre-ozone hole (1979-81) with the present values (1997-99) during springtime for the September-December period.	61
Figure 15- Interannual variation of the AOH contribution to the midlatitudes for the years 1997-2000. The plots are valid from September 1 to December 31.	62
Figure 16- Scatter plots between the midlatitude region (60°S-30°S) No PSC-PSC difference in total ozone and the normalized intensity of 100hPa geopotential height wave 1 and wave 2 for the September- October period.	63
Figure 17- Same as in Fig. 16 except for the November-December period.	64
Figure 18- Comparison of the midlatitudes (60°S-30°S) No PSC-PSC difference in total ozone with the normalized intensity of 100hPa geopotential height wave 1 and wave 2 at 60° S for the 1997-2000 September-December period.	65
Figure 19- Scatter plots between the polar regions (90°S-60°S) No PSC- PSC difference in total ozone and the normalized intensity of 100hPa geopotential height wave 1 and wave 2 for the September-October period.....	66
Figure 20- Same as in Fig. 19 except for the November-December period.	67
Figure 21- Comparison of the polar regions (90°S-60°S) No PSC-PSC difference in total ozone with the normalized intensity of 100hPa geopotential height wave 1 and wave 2 at 60° S for the 1997-2000 September-December period.....	68

1. INTRODUCTION

The dramatic decline in Antarctic ozone levels was first observed from the ozone data at Halley bay in 1983 (Farman et al. 1985). Every year since the 1980's, about two-thirds of ozone in the atmosphere is destroyed in the Antarctic lower stratosphere between the months of September and November (Hofmann et al. 1995). This phenomenon is called the ozone hole because the magnitude of the losses is large enough to thin out atmospheric ozone significantly. The science of the ozone hole has been an area of active research because of the significance of ozone in absorbing the harmful ultraviolet (UV-B) solar radiation. Long-term changes in surface UV-B radiation resulting from the depletion of the ozone layer is a source of international concern because of associated impacts on the biosphere. Ozone concentration and its distribution in the atmosphere have also proven to be important factors in climate change due to ozone-led stratospheric cooling (Shine 1986; Mahlman et al. 1994; WMO 1998; Randel and Wu 1999a; WMO 2002).

This study is aimed at addressing one such changing scenario in the global atmospheric ozone that affects the southern hemisphere midlatitudes - the Antarctic Ozone Hole (AOH). The effects of the AOH have been proven to extend to the sub-polar and midlatitude regions. Several studies have reported detection of very low ozone values over

Australia (Atkinson et al. 1989; Grainger and Karoly 2003) and South America (Kirchoff et al. 1996; Perez et al. 1998) during the southern hemisphere springtime. Some of such low ozone value days, referred to as low ozone events, have been recognized as effects of the AOH. The purpose of this research is to quantify the contribution of the AOH to the southern midlatitudes ozone budget between the years 1997-2000. The following subsection summarizes our current level of understanding of the processes involved in stratospheric ozone depletion.

a. Ozone

Ozone is present at all altitudes of the earth's atmosphere, but the bulk of it (~ 90%) resides in the stratosphere between 18 km to 50 km. The remaining ozone largely exists in the troposphere where it is an important component of photochemical smog.

Ozone is a trace constituent as it accounts for only 0.000004% of the entire atmospheric mass. Despite this fact, ozone plays a crucial role in absorbing harmful solar UV radiation, thus protecting the biosphere (Whitten and Prasad 1985). This absorption is also responsible for the observed increase in temperature between the tropopause and the stratopause via radiative mechanisms.

Atmospheric ozone measurements are typically reported as total ozone in a column of the atmosphere directly above a location. Total

ozone is measured in Dobson units (DU) and typically varies between 200 and 500 DU over the globe. A total ozone value of 500 DU is equivalent to 0.5 centimeters, the thickness of the ozone layer if it were brought down to the standard temperature and pressure of the Earth's surface. Global satellite measurements of daily total ozone from the Total Ozone Mapping Spectrometer (TOMS) have been made nearly continuously since 1978.

b. Stratospheric ozone: Chemistry and Dynamics

Atmospheric ozone is formed by the combination of atomic oxygen, O, and molecular oxygen, O₂. At altitudes above 20 km, production of O atoms results almost exclusively from the photodissociation of molecular O₂ by short wavelength radiation ($\lambda < 243$ nm). At lower altitudes, particularly in the troposphere, O atom formation from the photodissociation of nitrogen dioxide (NO₂) by longer wavelength UV radiation is more important. Ozone itself is photodissociated by both UV and visible light, but this reaction, together with the oxygen atom-oxygen molecule combination reaction, only serves to partition oxygen between O and O₃.

In the atmosphere, destruction of ozone is largely balanced by its production. It is now known that ozone in the stratosphere is removed predominantly by catalytic cycles involving homogeneous and

heterogeneous reactions of active free radical species in the HO_x, NO_x, ClO_x and BrO_x families (WMO 1985). Such species, with varying degrees, control the abundance and distribution of ozone in the stratosphere. In addition to chemical processes, dynamics also plays an important role in governing stratospheric ozone. The movement of ozone and its precursors, such as NO_x and CH₄, is largely governed by stratospheric dynamics. Researchers over the past two decades have developed a comprehensive theoretical picture of transport in the stratosphere (Andrews et al. 1987; McIntyre 1992; Randel and Newman 1997). One component of this picture is the Brewer-Dobson circulation (Fig 1), a zonally-averaged description comprising of air entering into the stratosphere through the tropical tropopause, ascending into the tropics and descending in the middle and high latitude winter hemisphere. This circulation is driven by vertically propagating planetary waves that originate from a combined influence of tropospheric topography features, meridional temperature gradients and the earth's Coriolis effect (Andrews et al. 1987; Holton et al. 1995; Hall and Waugh 1997). The evidence of this circulation can be seen from zonal mean distributions of ozone, other trace gases, temperatures, and zonal winds. The Brewer-Dobson circulation results in the transport of ozone poleward and downward into the extratropical stratosphere from its photochemical production region in the tropics.

c. Natural Ozone Variability

The natural variability of ozone occurs in a broad spectrum of both time and space scales. Atmospheric dynamics, chemistry and radiation, all play important roles in the variability of ozone (WMO 1998).

Long-term variations in ozone can be categorized into monthly, seasonal, annual and decadal cycles. Figure 2 shows the zonal mean distribution of stratospheric ozone mixing ratio as a function of altitude and latitude constructed using 5 years of data from the Microwave Limb Sounder (MLS) on the Upper Atmosphere Research Satellite (Atkinson 1993). The highest mixing ratios occur in the tropical middle to upper stratosphere, the ozone photochemical source region. Ozone concentrations decrease poleward and downward from the source region. The downward bulge seen at the mid-to-high latitude lower stratosphere is the result of poleward and downward advection from the tropical source region by the Brewer-Dobson circulation.

The seasonal evolution of zonal-mean total ozone is shown in Fig. 3 as a function of latitude. Despite the highest ozone-mixing ratio occurring in the tropical source region, total ozone values at the tropics are relatively low compared with the higher latitudes. The extratropical regions of both hemispheres show a large-amplitude annual cycle, with a maximum occurring after spring equinox near 70°N and 60°S. Thus, the

time mean and seasonal variations of ozone depend largely upon latitude as well.

During individual days, longitudinal variations in total ozone can also be considerably large (Andrews et al. 1987). Such short-term variations in ozone mainly originate from synoptic and sub-synoptic scale motions (Meetham 1937; Dobson et al. 1946; Atkinson 1997; WMO 1998). Figure 4 shows a picture of the temporal variability of ozone at five different locations during mid-October 1994. While the tropical total ozone shows a small degree of variability, midlatitudes have a much greater temporal variation.

d. Anthropogenic Ozone Variability

In the late 1960's and early 1970's, many important discoveries relating to atmospheric ozone were made as scientists began to investigate the potential impact of human activities on the stratosphere. Historically, the first such discovery was the catalytic loss of ozone from nitrogen oxides (NO_x) from a proposed fleet of supersonic transports (Johnston 1971). This was followed by the discovery of catalytic ozone loss from the space shuttle, which redefined the role of chlorine in the atmosphere (Stolarski and Cicerone 1974). At the same time, Sherry Rowland and Mario Molina, while studying the chemistry of chlorofluorocarbons (CFCs), discovered that although CFCs were inert in

the troposphere, they could be decomposed by UV radiation in the upper atmosphere (Molina and Rowland 1974). This implied that once transported to the stratosphere by atmospheric circulation, CFCs could release chlorine atoms that are capable of catalytically destroying ozone (Anderson et al. 1989).

CFCs are chemicals containing atoms of carbon, chlorine, and fluorine, and have been used in the manufacture of aerosol sprays, blowing agents for foams and packing materials. It is now well known that increasing levels of anthropogenic CFCs have contributed to the stratospheric ozone losses observed since the early 1980s (WMO 1985).

e. Antarctic Ozone Hole

Ever since the discovery of the dramatic ozone losses over Antarctica in the early 1980s, several independent data sets have confirmed the existence of an ozone-depleted region over Antarctica, referred to as the “ozone hole” (Chubachi and Kajawara 1986; Stolarski et al. 1986). Figure 5 shows the measured total ozone above Halley Bay station in Antarctica, where each point represents the average total ozone for the month of October between the years 1956-1995, and the thin lines represent the measurement uncertainty. The decline in October ozone values appears to have started in the mid-to-late 1970s, and by

1994, total ozone in October was less than half its value during the early 1970s.

The AOH is defined to exist when total ozone concentrations of less than 220 DU occur in the polar regions of the atmosphere (WMO 1995). As seen in Fig. 5, total ozone values in the Antarctic region before 1980s were typically around 300 DU. Since then, there has been a gradual decline in the Antarctic total ozone, with values below 100 DU observed in the 1990s.

Despite large interannual differences, a typical AOH life cycle begins in late August/early September, peaks by late September/early October, and recovers with the onset of the polar vortex breakup in late November/early December.

The AOH is characterized by the formation of the polar vortex, a large-scale cyclonic circulation occurring near 60°S during the winter months (Schoeberl and Hartmann 1991). An important ingredient to the ozone hole formation is the low temperature associated with the polar vortex. The temperature inside the vortex can be low enough to facilitate the formation of polar stratospheric clouds (PSCs). The formation of PSCs has been observed every winter in the Antarctic vortex core (Considine et al. 1994; Pawson et al. 1995; Pawson and Naujokat 1999; WMO 2002). The PSCs, combined with anthropogenic chlorine and the return of sunlight, form essential ingredients for the photochemical

reactions that are responsible for the observed springtime destruction of polar ozone.

Heterogeneous chemical reactions that occur on the PSCs are responsible for polar ozone depletion during the southern hemisphere spring (Solomon 1990). PSCs are divided into two types, Type 1 and Type 2. Type 1 PSCs are primarily frozen nitric acid trihydrate that form just above the frost point (about 195 K). They can be either solid or liquid, depending on the conditions. Type 2 PSCs are frozen H₂O (Turco et al. 1989), and are formed at much lower temperatures (e.g. 185 K at 25 km altitude). This is illustrated in Fig. 6, a time series of polar temperatures at 50 hPa showing the PSC formation thresholds in the southern hemisphere. The temperatures at which the two PSC types form differ by about 7 K, with Type 2 requiring lower temperatures than Type 1. In addition, during the 1978-2004 period, most of the PSC formation has occurred between the months of June and September.

It is now well known that PSC surfaces facilitate reactions of relatively long-lived chlorine compounds such as HCl, HOCl, and ClONO₂ that are not possible in the gas phase. These compounds are known to serve as reservoirs for chlorine liberated from the chlorofluorocarbons (Solomon et al. 1997). Ozone depletion rates are influenced largely by the chemical balance between such species and the ClO radical (Anderson et al. 1989).

Thus, the formation of the AOH is a combination of dynamical and chemical processes. While chemistry can influence the amount of polar ozone losses inside the vortex, processes such as vortex formation, evolution and breakup, also play an important role in the severity and extent of the AOH.

f. Impact of the AOH on Midlatitudes

Springtime Antarctic ozone depletion is substantial, with minimum values of about 100 DU seen every year since the early 1990s. As shown in Fig. 7, southern hemisphere midlatitude ozone values have declined since the 1980's, with the decline being greater in the Southern Hemisphere than the Northern Hemisphere (WMO 2002). Evidence shows that the observed decrease in the southern hemisphere midlatitudes total ozone has resulted from the combined effects of chemistry and dynamics of the AOH (Newman et al. 1997). For example, a significant component of the observed midlatitude total ozone changes have been attributed solely to the presence of Antarctic ozone depletion in 1987 (Atkinson and Plumb 1997). The dynamical break-up of the polar vortex can produce temporary local TCO reductions at specific midlatitudes locations (Atkinson 1993). The ozone-depleted polar vortex during some years has also been observed to pass over regions such as the southern tip of South America, producing elevated UV levels that

pose hazards to biological health. This provides an important motivation for studying the impacts of the AOH on southern midlatitudes.

Some of the southern midlatitude low ozone events resulting from the polar-midlatitudes transport have also occurred before the vortex breakup (Perez et al. 2000; Cordero and Grainger 2002). Despite the isolation of the polar vortex, cross-mass exchange from the polar vortex occurs during the winter-spring period (Juckes and McIntyre 1987; McIntyre 1989). A series of Chemical Transport Model (CTM) simulations for passive idealized tracers performed by Li et al. (2002) confirmed that vortex air can be exported from the Antarctic polar vortex to the middle latitudes by horizontal transport, even though vertical transport mechanisms dominate.

During the period 1997-2001, springtime total column ozone (TCO) amounts in the southern hemisphere midlatitudes (30°S-60°S) were ~ 6% below their pre-1980 values (WMO 2002). The TCO reduction in the midlatitudes can result from processes such as polar-midlatitude exchange, in-situ heterogeneous chemistry on liquid sulfate aerosols (Fahey et al. 1993), and tropopause height changes (McDermid et al. 1994). A 3-D CTM study has shown that an ozone reduction of 5% at 50°S can result from PSC-related depletion at the vortex edge (Chipperfield 1999). The equatorward transport of ozone has been observed to extend to 20°S latitude following the breakup of the polar

vortex (Eckman et al. 1996). Thus, the springtime depletion of the Antarctic ozone hole has potentially far-reaching effects making its quantification important.

In order to quantify the contribution of polar ozone depletion on midlatitudes, it is important to isolate the effects of polar ozone losses. This study aims to quantify the component of midlatitudes ozone changes that have occurred due to polar ozone reductions alone.

g. Interannual variability in Midlatitudes Ozone

Research based on both observations and model studies has revealed large interannual variability (IAV) in the size and evolution of the AOH, and this can affect year-to-year variability in midlatitude ozone levels via transport processes. The year-to-year differences in the TCO during the northern hemispheric polar night have been associated with IAV in planetary wave forcing (Kinnersley and Tung 1998). Stronger planetary wave forcing leads to high stratospheric temperatures and thus smaller ozone losses within the polar vortex (Newman et al. 2001, 2004). Planetary waves propagate through the troposphere and break in the stratosphere and higher levels (Haynes et al. 1991; Rosenlof and Holton 1993). The dissipation of these large-scale waves contributes to the zonal mean Brewer-Dobson circulation as discussed earlier.

Strong planetary wave forcing also contributes to a greater transport out of the polar vortex (Li et al. 2002). The results of Li et al. focused on the months of September-October, thus excluding the effects of ozone dilution after the polar vortex breakup. The influence of planetary waves on horizontal transport during the months of November-December is also likely to be important and requires further analysis.

Planetary wave forcing seemingly plays a dual role in determining the AOH contribution to the southern midlatitudes as summarized in Fig. 8. While stronger planetary waves produce lower polar ozone loss due to higher temperatures within the vortex, it also implies a greater transport out of the vortex itself, resulting in greater contribution to the midlatitudes. Thus, planetary wave strength (PWS) should be an important factor in influencing interannual variations seen in polar ozone depletion. Differences in polar ozone depletion, in turn, can produce interannual differences in midlatitude ozone variations through combined chemical and dynamical effects. While studies in the past have concentrated on the individual role of planetary waves, this study is aimed at understanding the dual role of planetary waves in determining midlatitudes ozone variations.

h. Project Goals

The aim of this study is to quantify the contribution of springtime polar ozone losses on southern midlatitude ozone values using a 3-D CTM. The difference between the model simulations is in the treatment of the polar chemistry, where one simulation will contain PSC-led heterogeneous chemistry and the other will not. The aim is to isolate the AOH contribution to the southern midlatitudes, and study the structure of the differences. Similar runs for four different years (1997-2000) have also been examined in order to establish any links between the AOH contribution to midlatitude ozone and PWS. In this part, the analysis of AOH contribution to midlatitude ozone for different years is accomplished by comparing the PSC-led polar and midlatitude ozone with intensities of 100hPa waves 1 and 2 at 60°S.

The next section explains the details of the model, its performance, and input/analysis datasets used in this study. This is followed by a results and discussion section, while the conclusions of the study are presented in the final section.

2. MODEL AND DATASETS

a. Description

Three-dimensional (3-D) CTMs are important tools for understanding the distribution of trace gas species and aerosols in the atmosphere (Rasch et al. 1994). The model used for the current study is an offline 3-D CTM, implying that it utilizes prescribed rather than predicted winds. This model has been used previously in both tropospheric and stratospheric studies. This includes simulations of stratospheric aerosols and long-lived tracers (Boville et al. 1991; Waugh et al. 1997), radioactive isotopes (Rasch et al. 1994), CFCs in the troposphere (Hartley et al. 1994), transport out of the Antarctic polar vortex (Li et al. 2002), and dissipation of the AOH (Li et al. 2002).

The transport components of the 3-D CTM are based on the National Center for Atmospheric Research's (NCAR's) Model of Atmospheric Transport and Chemistry (MATCH) (Mahowald et al. 1997a; Mahowald et al. 1997b; Rasch et al. 1997; Waugh et al. 1997). MATCH is based on the Middle Atmosphere Community Climate Model Version 2 (MACCM2) (Rasch et al. 1995), which is derived from its parent NCAR Community Climate Model Version 2 (CCM2) by extending the upper boundary to 75 km and by including chemistry and transport of trace constituents of the atmosphere (Plumb et al. 2000). The model utilizes

the shape-conserving, semi-Lagrangian advection scheme in which, a mass-fixer is applied after every advection time step to conserve tracer mass (Williamson and Rasch 1989; Rasch 1995).

The chemical components in the model are based on parameterized chemistry schemes for ozone production/loss rates from the NASA Goddard 2D model (Douglass et al. 1989). In addition to the homogeneous interactive gas phase chemistry, the NASA model also contains a parameterization of the heterogeneous reactions that occur on the surface of PSCs. These rates are incorporated in the model as coefficients that are functions of latitude, height and month of the year, and affect tracer fields as,

$$\frac{\partial \chi}{\partial t} = P - L\chi ,$$

where χ is the tracer-mixing ratio, and P and L are the production and loss coefficients respectively.

The PSC climatology, together with the other chemical and transport modules of the 3-D CTM, reproduces the AOH reasonably well. An observational comparison of model simulations is discussed in the next section.

b. Data Sources: Input and Analysis

The CTM used in this study, is driven by a set of assimilated data from the Upper Atmospheric Research Satellite (UARS) United Kingdom Meteorological Office (UKMO) global analyses (Swinbank and O'Neill 1994). The UARS UKMO assimilation data consists of daily averaged values of atmospheric temperature, geopotential height, zonal and meridional wind components, and vertical velocity. The data are gridded to a spatial resolution of 2.5 degrees latitude by 3.75 degrees longitude, which is equivalent to a spectral rhomboidal truncation of R56. The data are distributed at 22 pressure levels from 1000 hPa to 0.32 hPa (0 km to ~ 50 km), enabling a vertical coverage of the entire troposphere and stratosphere. The CTM simulations used in the present study have the same spatial resolution as the assimilation data, resulting in 96 longitudes, 72 latitude and 22 vertical levels.

The model is initialized using a global 3D ozone analysis field, Ozone Analysis System II (OASYS II), which determines the ozone field by statistical interpolation of combined satellite observations (Grainger and Cordero 2002). The OASYS data gives ozone-mixing ratios at 19 pressure levels between 100 hPa to 0.3 hPa, and has a horizontal resolution of 2.5X2.5 degrees. The OASYS data system has been validated against independent sets of observations, both surface-based

and in-situ ozonesonde data, details of which are discussed in Grainger and Cordero (2002). For this study, the OASYS data has been interpolated according to the resolution of the CTM.

The output analyses data required for this work were obtained from the Statistical and Climatological Analyses division of the National Center for Environmental Prediction (NCEP). National Aeronautics and Space Administration / Goddard Space Flight Center (NASA/GSFC) generates and maintains a set of stratospheric climate diagnostics, using data from the Climate Prediction Center (CPC) of NCEP. These diagnostics are used to track the behavior of the stratosphere in both hemispheres over the course of the year, and are available to the public via the internet. The 100 hPa wave 1 and wave 2 amplitudes of geopotential height at 60°S for the September-December period of 1997-2000 used in this study was obtained from the NCEP statistical and climatological analyses datasets.

c. Model Performance

The CTM simulations used in this study have previously been compared with observations (Li et al. 2003). The results of their study showed that the model simulates the day-to-day variations seen in TOMS observations at southern high latitudes very well. The CTM has also been shown to reproduce the midlatitude short-term variability and

seasonal trends observed in the ozonesonde data reasonably well (Grainger and Karoly 2003).

Similar comparisons of model simulations with observations are presented in this work. Figure 9 compares the modeled total ozone with observations on October 15 and November 18 of 1997. In general, the CTM total ozone values are lower than the observations for the entire run period. This is due to the fact that the initial ozone mixing ratio values obtained from OASYS do not include the tropospheric ozone component. However, the model successfully replicates vortex formation and split on October 15 and November 18 with precise accuracy.

Thus, the model driven by assimilated UKMO winds each year captures the polar vortex evolution, dissipation and the total ozone values in the polar/midlatitudes regions with considerable accuracy. The modeled ozone-mixing ratio is also compared with the ozonesonde profiles during September at 54°S, 158°E. As shown in Fig. 10, the model is able to capture the ozone profile reasonably well. The close correspondence of model output with observations obtained in this study as well as previous studies (Li et al. 2003; Grainger and Karoly 2003) reaffirms its validity in representing large-scale horizontal flow.

d. Model Simulations

The model is initialized at 1200UTC on September 1, and run through December 31 with a one-hour time step for the different years, 1997-2000. The model output is saved every 24 hours yielding 122 days of ozone mixing ratio values for the September-December run period. The isolation of the AOH contribution to midlatitudes ozone is achieved by performing two runs with the CTM. First is the default run called the PSC run. In this simulation, the CTM uses chemistry from the NASA P/L rates, which includes PSC chemistry in the high latitude winter/spring period. The second run, referred as No-PSC run hereafter, uses a modified chemistry obtained by adjusting the NASA 2D P/L rates towards the P/L rates obtained from the CSIRO Telecommunications and Industrial Physics (CTIP) model that has no PSC chemistry. Even though the extent of the PSC formation varies from year to year, PSC-related chemistry is most common between the altitudes of 12 km to 20 km (Schoeberl and Hartmann 1991). Thus, the alteration of the P/L rates is restricted to the altitudes between 12km to 20km and the latitudes between 90°S -60°S. The P/L rates in the midlatitude region (60°S -30°S) are unaltered for the No-PSC run. Figure 11 shows the production and loss Coefficients of the NASA 2-D model with and without PSC

modifications at 12 km on September 15. The climatological PSC P/L rates used in the model are the same for all the years 1997-2000, and thus the present simulations do not capture the interannual differences in the temperature-initiated/PSC chemical changes in polar ozone. However, this is not expected to alter the validity of the results presented here, as this study focuses on the dynamical aspects of polar-midlatitude ozone variations.

3. RESULTS AND DISCUSSION

The AOH contribution to the southern midlatitudes is quantified using two simulations with differing P/L rates as described in the previous section. The P/L rates are based on a PSC climatology, and thus prevent the inclusion of temperature-led polar ozone loss variations between the various years. Thus, any interannual variations produced in the model-simulated polar ozone values must be of dynamical origin.

a. Impact on midlatitudes

The total ozone difference between the No-PSC and PSC runs in the midlatitudes (60°S-30°S) for the years 1997-2000 is shown in Fig. 12. This difference represents the midlatitude total ozone contribution coming from the AOH alone, and is referred to as the midlatitude AOH factor (MAF) hereafter. In general, the AOH makes a significant

contribution to midlatitude TCO in all years. After the model initialization on September 1, there is a sharp increase in the MAF during the first few days. This sharp increase lasts for ~ 20 days in the 60°S-50°S region. At lower latitudes, the magnitude of the change is delayed and does not have such large values. This initial sharp increase is expected because the difference between the two runs is begins at zero; and thus, the first 10 days are not considered in subsequent calculations.

The MAF exhibits an increasing trend from the model initialization period, reaching a maximum in the October-November period before it begins to decrease in the month of December. While the MAF maximum corresponds to the periods of greatest polar ozone losses, the decrease seems to be associated with the polar vortex breakup and the eventual mixing of ozone rich air into the midlatitudes.

MAF values averaged over the September-December period for the various midlatitude regions 60°S-50°S, 50°S-40°S and 40°S-30°S, and 60°S-30°S during 1997-2000 are summarized in Table 1. As expected, the 60°S-50°S region is most affected by the polar ozone losses, while the 40°S-30°S region gets the least contribution from the polar regions. It is evident from Fig. 12 that the 60°S-50°S region exhibits a greater day-to-day variability compared to the 50°S-40°S and 40°S-30°S regions during

all years. Thus, the midlatitude regions closest to the polar vortex are most susceptible to polar ozone changes originating from PSC chemistry.

There is also a large month-to-month variation in the MAF during all the years, as shown in Table 2. Averaged over four years (1997-2000), the September-October period exhibits only about $\sim 27\%$ decrease in midlatitudes ozone due to polar air intrusion, while $\sim 57\%$ decrease occurs during the November-December period. A higher November-December polar contribution to midlatitude ozone reveals the importance of transport processes during these months as well.

Averaged between 1997-2000, the overall midlatitude (60°S - 30°S) MAF during the September-December season is $\sim 41\%$ of the PSC-initiated total polar ozone losses. In other words, for every 100 DU of PSC-related total polar ozone losses, a loss of 41 DU occurred in the midlatitudes during the 1997-2000 period. The MAF for the September-October period is found to be $\sim 27.5\%$, consistent with the results reported in Li et al. (2002). Since the MAF obtained in our study is an equivalent representation of the vortex mass outflow, the higher estimate of $\sim 41\%$ obtained can be explained by the fact that it includes the months November and December. The months of November and December usually correspond to the breakup of the polar vortex, increasing the possibility that remnants of the ozone hole are transported

to the southern midlatitudes. The inclusion of these months therefore is significant in determining the AOH contribution to the midlatitudes.

The percent total ozone deviations for the various midlatitude regions obtained from the CTM during the September-December period for the years 1997-2000 is shown in Fig. 13. This was calculated by dividing the PSC and No-PSC total ozone differences by the PSC total ozone in the midlatitude region. The observed sharp decline in the total ozone deviation during the first 10 days is removed from further calculations.

The average decrease resulting from the transport of low polar ozone air to midlatitudes (60°S-30°S) for the September-December period ranges between -2.5% in 1999 to -4.9% in 2000, the maximum deviations range between -10% in 2000 and -5.5% in 1999. The modeled average and maximum ozone deviations values are listed in Table 3.

In order to further explore the effects of polar ozone loss on midlatitudes, CTM midlatitude total ozone deviations are compared with TOMS observations. The results for 1997-2000 is compared with TOMS data expressed as a (1997-2000) deviation from pre-ozone hole (1979-86) midlatitude TCO values, and are shown in Fig. 14. The observed springtime (September-December) decline in southern midlatitude TCO between the 1997-2000 period is ~ 6.4%, consistent with the reported trends (WMO 2002). The average decline obtained from the difference between CTM PSC and No-PSC runs, for the same period is ~ 3.7 %.

Thus, averaged between the years 1997-2000, PSC-initiated polar ozone losses account for about 61% of the total observed springtime midlatitudes ozone decline.

The observed maximum ozone deviations are also found to be greater than the modeled maximum deviations for all the midlatitude regions examined (60°S-50°S, 50°S-40°S and 40°S-30°S) during the September-December period (Table 4). The PSC-related midlatitude TCO deviations, during the 1997-2000 period, account for ~ 73% of the observed deviations in the 60°S-50°S region, ~ 65% in the 50°S-40°S region and 64% in the 40°S-30°S region.

Also shown in Table 4 are the dates corresponding to the maximum midlatitude TCO deviation obtained from the model runs. In general, the maximum deviations in all latitude regions occur during the months of November and December. These months usually mark the breakup of polar vortex following which the low ozone air from the polar regions eventually is mixed to lower latitudes.

The above analysis has also shown that there is a large IAV in both the average and maximum midlatitude ozone deviation obtained from PSC-related polar ozone losses alone. The next section analyzes these interannual variations in order to define the role of extratropical planetary waves in producing dynamically-induced midlatitude ozone changes.

b. Interannual Variability

The September-December average MAF for the years 1997-2000 are compared in Fig. 15. This is calculated by averaging the total ozone difference between the No-PSC and PSC runs for the September-December period. As seen in the figure, a large year-to-year variation exists in midlatitude ozone depletion due to the AOH. While the year 1999 has the least (~ 6.4 DU) midlatitudes contribution, 2000 has the highest contribution (~ 13.4 DU). In terms of polar ozone losses, the years 1997-1999 (range: ~ 22.4 DU to ~ 23.4 DU) had comparable losses, while the value in 2000 was much greater (~ 27.3 DU). However, midlatitude ozone changes are different in 1998 (~ 9.1 DU) and 1999 (~ 6.4 DU), despite their similar polar losses (~ 22.4 DU). As previously, discussed, planetary waves of tropospheric origin can influence the midlatitude ozone variations by controlling both polar ozone losses and transport of polar air into the midlatitudes.

A useful way to study planetary wave behavior is by the analysis of isobaric geopotential height surfaces in the upper troposphere or lower stratosphere. Undulations in the isobaric geopotential height field are manifestations of planetary wave activity (Andrews et al. 1987). Southern midlatitude temperature and ozone data between 17 and 63 km have been shown to have a wave two signature during the month of August (Barnet and Corney 1984; Ward et al. 2000). However, past

studies have revealed the importance of both wave 1 and 2 in southern hemisphere wave driving (Hartmann et al. 1984). Thus, analysis of planetary waves of zonal wavenumbers 1 and 2 can help explain their influence on polar-midlatitudes transport processes.

In order to understand the role of extratropical planetary waves in controlling midlatitude ozone variations, interannual variations in the 100 hPa wave amplitudes of zonal wavenumbers 1 and 2 at 60°S are analyzed and compared with the MAF for 1997-2000.

Planetary Waves and Horizontal transport

Scatter plots of monthly-averaged 100 hPa wave 1 and wave 2 intensities (normalized) at 60°S and the MAF for the years 1997-2000, are shown in Figs. 16 and 17, and are summarized in Table 5. A small correlation obtained between the wave amplitudes and MAF indicates that there are factors other than wave amplitudes that affect the polar-midlatitudes transport processes. The line shown in the figures represents a linear best fit between the two data sets. The normalized intensities of both waves 1 and 2 are positively correlated with the MAF during the September-October period. As shown in Fig. 16, wave 1 has a higher correlation (0.41) than wave 2 (0.21), indicating the greater importance of wave 1 in controlling polar-midlatitude ozone transport during the September-October period. However, during the November-December period, wave 1 shows a weak negative correlation (-0.17) while

wave 2 is strongly correlated (0.77) with the MAF (Fig. 17). As mentioned above, the months of November and December usually correspond to the breakup of the polar vortex, thereby increasing wave-induced transport of ozone-poor polar air into the midlatitudes.

Thus, while the 100 hPa wave 1 has a greater dynamic significance before the vortex breakup (September-October), the 100 hPa wave 2 is an important controlling factor after the breakup of the polar vortex (November-December) and possibly before the breakup as well.

This can also be demonstrated by comparing the daily values of MAF for 60°S-30°S with normalized wave intensities for the individual years 1997-2000, as shown in Fig. 18. Of the four years 1997-2000, November-December wave 2 intensity is smallest in 1999 (Fig. 18c) and largest in 2000 (Fig. 17d). Correspondingly, the highest November-December MAF was observed in 2000, and the lowest in 1999 during these months. The years 1997 and 1998 show a similar consistency in the MAF and the relative strength of wave 2 intensities. This suggests that wave 1 is less important as a transport-controlling factor for the period of November-December than wave 2.

Thus, wave 2 has a larger contribution to horizontal transport of air out of the polar vortex mass compared with wave 1 during the November-December period, while during the months of September-

October, both waves 1 and 2 can be important in transporting mass out of the polar vortex.

Planetary Waves and Polar Ozone

In order to more clearly determine the role of planetary waves in controlling polar ozone, normalized intensities of wave 1 and 2 are compared with PSC-initiated polar ozone losses for the years 1997-2000. These losses for each year are calculated by taking the difference between the CTM NO-PSC and PSC run total ozone values at the regions between 90°S-60°S. As shown in Fig. 19, wave 1 has a positive correlation (~ 0.4), while wave 2 is very poorly correlated with polar ozone losses during the September-October months (Table 5). However, during the November-December months (Fig. 20), wave 1 is negatively correlated (-0.3) and wave 2 has a positive correlation (0.6).

A positive correlation obtained between polar ozone losses and wave intensities in this analysis implies that stronger waves contribute to higher polar ozone losses resulting from PSC chemistry alone. This however, contradicts the current understanding of planetary wave influence on PSC-led polar ozone losses since stronger waves are expected to cause smaller polar ozone losses. A positive correlation between polar ozone losses, and wave intensities can also result from the

transport of ozone-deficient air from the midlatitudes to the polar regions.

In order to examine the above contradictory results, the wave intensities are compared with the CTM-generated polar ozone losses for individual years. As shown in Fig. 21, the polar ozone losses in general exhibit an increasing trend until October, when they decline for all years except 2000. In 2000, polar ozone losses show an increasing trend in the month of December as well. An analysis of waves 1 and 2 in 2000 suggests that the strong wave 2 amplitudes during the November-December period of 2000 contribute to the trend shown in Fig. 20.

Also seen in Fig. 21 (d) is a weak wave 1-strong wave 2 pattern in the November-December period that is unique to 2000; the years 1997-1999 show strong wave 1-weak wave 2 trends for the same period. This also suggests that waves 2 and 1 can have a combined influence in determining polar ozone losses via transport processes during the November-December period.

The potential role of planetary waves in controlling PSC-led polar ozone losses is restricted in our study due to the absence of temperature-PSC chemistry feedbacks in the model simulations. However, this study suggests a much greater month-to-month variation in the role of waves 1 and 2 in influencing springtime polar ozone losses than has been shown by previous studies. The combined effect of these waves, especially after

the vortex breakup, can also influence polar ozone by controlling transport mechanisms.

4. CONCLUSIONS

The contribution of springtime polar ozone depletion to the declining trends of midlatitude ozone is investigated using a series of CTM simulations performed for the years 1997-2000. The CTM, driven by offline-assimilated winds, is able to replicate interannual variations in the formation of the vortex, its evolution, breakup and the amount of ozone loss inside the polar vortex with considerable accuracy. By changing the polar chemistry, two runs are performed, one with PSC chemistry and one without. This allows for the isolation of the effects of springtime polar ozone losses on midlatitude ozone variations. The results of these simulations show that when averaged over the period between 1997-2000, a decline of approximately 3.7% in midlatitudes TCO can be attributed to PSC-initiated polar ozone losses. The observed change in midlatitude TCO, as measured by TOMS, is approximately 6%, and thus the polar ozone losses account for around ~ 61% of the midlatitude ozone decline. The remaining 39% are likely a result of other processes such as tropospheric height changes or in-situ chemistry.

The average November-December PSC-led changes in midlatitude TCO for the 1997-2000 period are found to be higher than during September-October. This is likely due to exceptionally large changes in November-December during 2000, suggesting that transport processes

responsible for polar-midlatitude exchanges are important even after the vortex breakup. The springtime midlatitude ozone resulting from the polar decline is greatest (- 4.9%) in 2000 and smallest (-2.5%) in 1999.

There is an equatorward decrease in influence of polar chemistry on the day-to-day midlatitudes ozone variability. The average and maximum deviation in the midlatitude TCO resulting from the PSC-led polar ozone losses in general is found to decrease equatorward.

It was also found that there is a large IAV in the PSC-initiated midlatitude ozone variations associated with IAV in extratropical planetary wave activity. These variations originate from an apparent overlap in the role of extratropical planetary waves. Planetary waves appear to control the polar-midlatitude horizontal transport, and produce the observed IAV in the springtime polar-midlatitude ozone variations.

The amplitudes of the extratropical planetary waves of both zonal wave numbers 1 and 2 are important in controlling the springtime midlatitudes ozone in the Southern Hemisphere. While wave 1 is more important in polar-midlatitudes transport during September-October, wave 2 is more significant in November-December, although its role in the months of September-October cannot be completely neglected.

In terms of affecting polar ozone, wave 2 seems to be more important during the months of November-December, while wave 1 is significant in the September-October period. The combined influence of

waves 1 and 2 in controlling polar ozone losses, especially after the polar vortex breakup, can be an important factor. This study, thus has characterized the significance of extratropical planetary wave amplitudes in producing the AOH-related midlatitude ozone variations. However, other features such as the residual circulation can influence transport processes between the polar and midlatitude regions. The absence of the polar temperature-ozone feedback in our chemistry module is a limitation in the present analysis. The modeled year-to-year variations in polar ozone losses thus incorporate only the dynamical factors that produce these changes.

REFERENCES

- Anderson, J. G., W. H. Brune, and M. H. Proffitt, 1989: Ozone destruction by chlorine radicals within the Antarctic vortex: The spatial and temporal evolution of ClO-O₃ anticorrelation based on *in situ* ER-2 data. *J. of Geophys. Res.*, **94 (D)**, 11,465-11,479.
- Andrews, D. G., J. R. Holton, C. B. Leovy, 1987: *Middle Atmosphere Dynamics*, Academic Press Inc., London, 483pp.
- Atkinson, R. J., W. A. Mathews, P. A. Newman, and R. A. Plumb, 1989: Evidence for the mid-latitude impact of Antarctic ozone depletion. *Nature*, **340**, 290-293.
- , 1993: An observational study of the austral spring stratosphere: dynamics, ozone transport and the “ozone dilution effect”. Sc.D. thesis, Mass. Instit. Of Technol, 386pp.
- , 1997: Ozone variability over the southern hemisphere. *Aust. Met. Mag.*, **46**, 195-201.
- , and R. A. Plumb, 1997: Three-dimensional ozone transport during the ozone hole breakup in December 1987. *J. Geophys. Res.*, **102**, 1,451-1,466.
- Barnett, J. J., and M. Corney, 1984: Temperature comparisons between the NIMBUS 7 SAMS, rocket/radiosondes and NOAA-6 SSU. *J. Geophys. Res.*, **89**, 5,294-5,302.
- Boville, B. A., J. R. Holton, and P. W. Mote, 1991: Simulation of the Pinatubo aerosol cloud in a general circulation model. *Geophys. Res. Lett.*, **18**, 2,281-2,284..
- Bojkov, R. D., 1986: The 1979-85 ozone decline in the Antarctic as reflected in ground based observations. *Geophys. Res. Lett.*, **13**, 1,236-1,239.
- Cordero, E. C., and S. Grainger, 2002: Low ozone concentrations over Macquarie Island during 1997. Part I: trajectory analysis. *Aust. Met. Mag.*, **52**, 85-94.

- Chapman, S., 1930: A theory of upper atmospheric ozone. *Roy. Meteor. Soc. Mem.*, **3**, 103-125.
- Chipperfield, M. P., 1999: Multiannual simulations with a three-dimensional chemical transport model. *J. Geophys. Res.*, **104**, 1,781-1,805.
- Chubachi, S., and R. Kajawara, 1988: Total ozone by lunar Dobson observation at Syowa, Antarctica. *Geophys. Res. Lett.*, **15**, 905-906.
- Considine, D. B., A. R. Douglass, and C. H. Jackman., 1994: Effects of a polar stratospheric cloud parameterization on ozone depletion due to stratospheric aircraft in a two-dimensional model. *J. Geophys. Res.*, **99**, 18,879-18,894.
- Dobson, G. M. B., A. W. Brewer, and B. M. Cwiling: 1946: Meteorology of the lower stratosphere. *Proc. Roy. Meteorol. Soc. London*, **A185**, 144-175.
- Douglass, A. R., C. H. Jackman, and R. S. Stolarski, 1989: Comparison of model results transporting the odd nitrogen family with results transporting separate odd nitrogen species. *J. Geophys. Res.*, **94**, 9,862-9,872.
- Eckman, R. S., W. L. Grose, D. E. Turner, and W. T. Blackshear, 1996: Polar ozone depletion: A 3-dimensional chemical modeling study of its long-term global impact. *J. Geophys. Res.*, **101**, 22,977-22,989.
- Fahey, D. W., S. R. Kawa, E. L. Woodbridge, P. Tin, J. C. Wilson, H. H. Jonsson, J. E. Dye, D. Baumgardner, S. Borrmann, D. Toohey, L.M. Avalone, M. H. Proffitt, J. Margitan, M. Loewenstein, J. R. Podolske, R. J. Salawitch, S. C. Wofsy, M. K. W. Ko, D. E. Anderson, M. R. Schoeberl, K. K. Chan., 1993: In situ measurements constraining the role of sulphate aerosols in mid-latitude ozone depletion. *Nature*, **363**, 509-514.
- Farman, J. C, B. G. Gardiner and J. D. Shanklin, 1985: Large losses of total ozone in Antarctica reveal seasonal ClO_x/NO_x interaction. *Nature*, **315**, 207-210.

- Grainger, S. and E. C. Cordero, 2002: Low ozone concentrations over Macquarie Island during 1997. Part II: satellite ozone analysis. *Aust. Met. Mag.*, **51**, 95-106.
- Grainger, S., and D. J. Karoly, 2003: A transport model study of the breakup of the Antarctic ozone hole in November 2000. *Geophys. Res. Lett.*, **30**, 1,368.
- Hall, T. M. and D. W. Waugh, 1997: Timescales for the stratospheric circulation derived from tracers. *J. Geophys. Res.*, **102**, 8,991-9,001.
- Hartley, D. E., D. L. Williamson, P. J. Rasch, and R. Prinn, 1994: Examination of tracer transport in the NCAR CCM2 by comparison of CFC13 simulations with ALE/GAGE observations. *J. Geophys. Res.*, **99**, 12,855– 12,896.
- Hartmann, D. L., C. R. Mechoso, and K. Yamazaki, 1984: Observations of Wave-Mean Flow Interaction in the Southern Hemisphere. *J. Atmos. Sci.*, **41**, 351–362.
- Haynes, P. H., C. J. Marks , M. E. McIntyre, T. G. Shepherd, K. P. Shine, 1991: On the "downward control" of extratropical diabatic circulations by eddy-induced mean zonal forces. *J. Atmos. Sci.*, **48**, 651-678.
- Hofmann, D. J., S. J. Oltmans, B. J. Johnson, J. A. Lathrop, J. M. Harris, and H. Vömel, 1995: Recovery of ozone in the lower stratosphere at the South Pole during the spring of 1994. *Geophys. Res. Lett.*, **22**, 2,493-2,496.
- Holton, J. R., P. H. Haynes, M. E. McIntyre, A. R. Douglass, R.B. Rood, and L. Pfister, 1995: Stratosphere-troposphere exchange. *Rev. Geophys.*, **33**, 403-439.
- Juckes, M. N., and M. E. McIntyre, 1987: A high resolution, one-layer model of breaking planetary waves in the stratosphere. *Nature*, **328**, 590-596.
- Johnston, H., 1971: Reductions of Stratospheric Ozone by Nitrogen Oxide Catalysts from Supersonic Transport Exhaust. *Science*, **173**, 517.

- Kirchoff, V. W. J. H., N. J. Schuch, D. K. Pinheiro, and J. M. Harris, 1996: Evidence of an ozone hole perturbation at 30° south. *Atmos. Environ.*, **30**, 1,481-1,488.
- Kinnersley, J. S., and K. K. Tung, 1998: Modeling the Global Interannual Variability of Ozone Due to the Equatorial QBO and to Extratropical Planetary Wave Variability. *J. Atmos. Sci.*, **55**, 1,417-1,428.
- Labitzke, K., 1982: On interannual variability of the middle stratosphere during northern winters. *J. Meteorol. Soc. Japan*, **60**, 124.
- Li, S., E. C. Cordero, and D. J. Karoly, 2002: Transport out of the Antarctic polar vortex from a three-dimensional transport model. *J. Geophys. Res.*, **107**, (D11), 4132, DOI: 10.1029/2001JD000508.
- , ———, and ———, 2003: Three-dimensional simulations of springtime dissipation of the Antarctic ozone hole. *Aust. Met. Mag.*, **52**, 1-9.
- Mahlman, J. D., J. P. Pinto, and L. J. Umscheid, 1994: Transport radiative and dynamical effects of the Antarctic ozone hole: A GFDL SKYHI model experiment. *J. Atmos. Sci.*, **51**, 489-508.
- Mahowald, N. M., R. G. Prinn, and P. J. Rasch, 1997a.: Deducing CCl₃F emissions using an inverse method and chemical transport models with assimilated winds. *J. Geophys. Res.*, **102**, 28,153-28,168.
- Mahowald, N. M., P. J. Rasch, B. E. Eaton, S. Whittlestone, and R. G. Prinn, 1997b: Transport of ²²²radon to the remote troposphere using the Model of Atmospheric Transport and Chemistry and assimilated winds from ECMWF and the National Center for Environmental Prediction/NCAR. *J. Geophys. Res.*, **102**, 28,139-28,152.
- McDermid, I. S., M. Schmoe, E. W. Sirko and T. D. Walsh, 1994: Lidar Measurements of Stratospheric Ozone, Temperature, and Aerosol Profiles at Mauna Loa, NOAA Climate Monitoring and Diagnostics Laboratory No. 22, Summary Report 1993. 125-127.
- McIntyre, M. E., 1992: *The Use of EOS for Studies of Atmospheric Physics*, 313-386.

- Meetham, A. R., 1937: The correlation of the amount of ozone with other characteristics of the atmosphere. *Quart. J. Roy. Meteorol. Soc.*, **63**, 289-307.
- Molina, M. J., and F. S. Rowland, 1974: Stratospheric Sink for Chlorofluoromethanes: Chlorine Atom-Catalyzed Destruction of Ozone. *Nature*, **249**, 810.
- McIntyre, M. E., 1989: On the Antarctic ozone hole. *J. Atmos. Terr. Phys.*, **51**, 29-43.
- NCEP Statistical and Climatological Analyses (1997-2000):
[Available on-line at: <http://code916.gsfc.nasa.gov>]
- Newman, P. A., J. Gleason, R. McPeters, and R. Stolarski, 1997: Anomalous low ozone over the arctic. *Geophys. Res. Lett.*, **24**, 2,689-2,692.
- , E. R. Nash, and S. R. Kawa, 2004: What controls the size of the Antarctic ozone hole? 12th Conference on the Middle Atmosphere.
- , E. R. Nash, and J. E. Rosenfield, 2001: What controls the temperature of the Arctic stratosphere during the spring? *J. Geophys. Res.*, **106**, 19,999 – 20,010.
- Pawson, S. and B. Naujokat, 1999: The cold winters of the middle 1990s in the northern lower stratosphere. *J. Geophys. Res.*, **104**, 14,209-14,222.
- , B. Naujokat, and K. Labitzke, 1995: On the polar stratospheric cloud formation potential of the northern stratosphere. *J. Geophys. Res.*, **100**, 23,215-23,225.
- Perez, A., E. Crino, A. de Carcer, and F. Jaque, 2000: Low-ozone events and three-dimensional transport at midlatitudes of South America during springs of 1996 and 1997. *J. Geophys. Res.*, **105**, 4,553-4,561.
- , I. Aguirre de Carcer, J. O. Tocho, E. Crino, H. F. Ranea Sandoval, M. E. Berni, L. Da Silva, D. Henriques, F. Cusso, and F.

- Jaque, 1998: The extent of ozone hole over South America during the spring of 1993,1994 and 1995. *J. Phys. D Appl. Phys.*, **31**, 812-819.
- Plumb, I., R. Law, D. Waugh and R. Dargaville, 2000: Description of the CRC 3-D CTM, 4-6.
- Randel, W. J., and F. Wu, 1999a: Cooling of the Arctic and Antarctic polar stratospheres due to ozone depletion. *J. Clim.*, **12**, 1,467-1,479.
- and P. A. Newman, 1997: The stratosphere in the southern hemisphere, CRC for Southern Hemisphere meteorology Tech reports No.2.
- Rosenlof, K. H., and J. R. Holton, 1993: Estimates of the stratospheric residual circulation using the downward control principle. *J. Geophys. Res.*, **98**, 10,465-10,479.
- Rasch, P. J., B. A. Boville, and G. P. Brasseur, 1995: A three-dimensional general circulation model with coupled chemistry for the middle atmosphere, *J. Geophys. Res.*, **100**, 9,041– 9,071.
- , N. M. Mahowald, and B. E. Eaton, 1997: Representations of transport, convection and the hydrologic cycle in chemical transport models: Implications for the modeling of short lived and soluble species. *J. Geophys. Res.*, **102**, 28,127-28,138.
- , X. Tie, B. A. Boville, and D. L. Williamson, 1994: A three-dimensional transport model for the middle atmosphere. *J. Geophys. Res.*, **99**, 999-1,017.
- Schoeberl, M. R., and D. L. Hartmann, 1991: The dynamics of the stratospheric polar vortex and its relation to springtime ozone depletion. *Science*, **251**, 46-52.
- Shine, K. P., 1986: On the modeled thermal response of the Antarctic stratosphere to a depletion of ozone. *Geophys. Res. Lett.*, **13**, 1331-1334.
- Stolarski, R. S., and R. J. Cicerone, 1974: Stratospheric Chlorine: A Possible Sink for Ozone. *Can. J. Chemistry*, **52**, 1610.

- , A. J. Krueger, M. R. Schoeberl, R. D. McPeters, P. A. Newman, J. C. Alpert, 1986: Nimbus 7 satellite measurements of the springtime Antarctic ozone decrease. *Nature*, **322**, 808-811.
- Solomon, S., 1990: Progress towards a quantitative understanding of Antarctic ozone depletion. *Nature*, **347**, 347-353.
- , S. Bormann, R. R. Garcia, R. Portmann, L. Thomason, L. R. Poole, D. Winkler and M. P. McCormick, 1997: Heterogeneous chlorine chemistry in the tropopause region. *J. Geophys. Res.*, **102**, 21,411-21,429.
- Swinbank, R., and A. O'Neill, 1994: A stratosphere-troposphere data assimilation system. *Mon. Weather Rev.*, **122**, 686– 702.
- Turco, R. P., O. B. Toon, and P. Hamill, 1989: Heterogeneous physicochemistry of the polar ozone hole. *J. Geophys. Res.*, **94**, 16493-16510.
- Ward, W. E., J. Oberheide, M. Riese, P. Preusse, and D. Offermann, 2000: Planetary Wave Two Signatures in CRISTA-2 Ozone and Temperature Data, *Geophys. Monograph*, **123**, 319-325.
- Waugh, D. W., T. M. Hall, W. J. Randel, P. J. Rasch, B. A. Boville, K. A. Boering, S. C. Wofsy, B. C. Daube, J. W. Elkins, D. W. Fahey, G. S. Dutton, C. M. Volk, P. F. Vohralik, 1997: Three-dimensional simulations of long-lived tracers using winds from MACCM2. *J. Geophys. Res.*, **102**, 21,493 – 21,513.
- Whitten, R. C. and S. S. Prasad, 1985: *Ozone in the free atmosphere*. Van Nostrand Reinhold Company, New York, 283 pp.
- Williamson, D. L. and P. J. Rasch, 1989: Two-dimensional semi-Lagrangian transport with shape-preserving interpolation. *Mon. Weather Rev.*, **117**, 102-129.
- WMO, 1985: Atmospheric Ozone. Global Ozone Research and Monitoring Project-Report No. **16**, Geneva.
- , 1998: Scientific Assessment of Ozone Depletion, Global Ozone Research and Monitoring Project-Report No. **44**, Geneva.

_____, 2002: Scientific Assessment of Ozone Depletion. Global Ozone Research and Monitoring Project-Report No. **47**, Geneva.

Table 1 - Difference in total ozone between PSC and No PSC run, in DU, for the polar regions (averaged between 90°S-60°S), the midlatitudes (averaged between 60°S and 30°S) and for the different midlatitudes regions (60°S-50°S, 50°S-40°S, 40°S-30°S), for the years 1997-2000.

Year	Difference in total Ozone between PSC and NOPSC runs (in DU)				
	90°S-60°S	60°S-30°S	60°S-50°S	50°S-40°S	40°S-30°S
1997	23.4	11.5	15.4	10.9	8.3
1998	22.4	9.14	12.3	8.5	6.5
1999	22.4	6.4	9.3	5.6	4.3
2000	27.3	13.4	17.2	12.8	10.1

Table 2 - Difference in total ozone between PSC and No PSC run, in DU, for the midlatitudes (averaged between 60°S and 30°S) (MAF) for individual months between September and December during 1997-2000.

Year	Midlatitudes AOH factor averaged between 60°S and 30°S (in DU) for			
	September	October	November	December
1997	4.6	11.1	15.7	15.1
1998	3.3	8.7	12.4	12.2
1999	3.0	6.9	8.1	7.5
2000	3.7	11.2	19.8	19.1
Average	3.6	9.5	14.0	13.4

Table 3 - Average and maximum deviation from NO-PSC chemistry in the modeled midlatitude (60°S- 30°S) total ozone (in %), for the years 1997-2000.

Year	Average midlatitudes (60°S-30°S) total ozone deviations from the PSC/No PSC CTM runs for Sept-Dec (in %)	Maximum midlatitudes (60°S-30°S) total ozone deviations from the PSC/No PSC CTM runs for Sept-Dec (in %)
1997	-4.2	-6.6
1998	-3.2	-5.0
1999	-2.5	-3.8
2000	-4.9	-8.2

Table 4 - Comparison of the modeled maximum midlatitude (60°S-30°S) total ozone deviation with the TOMS present /pre-ozone hole maximum midlatitude (60°S-30°S) total ozone deviation for the for September-December period of 1997-2000.

Year	% Maximum Midlatitudes (60°S-30°S) Total Ozone deviation for Sept-Dec period obtained from					
	TOMS (1979-80)-present for			CTM (NOPSC-PSC) for		
	60°S-50°S	50°S-40°S	40°S-30°S	60°S-50°S	50°S-40°S	40°S-30°S
1997	-9.8 (Dec 5)	-9.1 (Dec 10)	-9.3 (Nov 20)	-8.8 (Dec 5)	-6.4 (Dec 10)	-4.7 (Nov 20)
1998	-10.8 (Sep 27)	-10.4 (Dec 15)	-6.2 (Dec 12)	-6.0 (Sep 27)	-5.0 (Dec 15)	-4.0 (Dec 12)
1999	-10.6 (Oct 30)	-9.1 (Dec 16)	-6.5 (Dec 10)	-5.5 (Oct 30)	-3.5 (Dec 16)	-2.6 (Dec 10)
2000	-9.5 (Nov 30)	-6.9 (Nov 13)	-6.6 (Nov 21, 22, 23)	-9.8 (Nov 30)	-8.1 (Nov 13)	-6.9 (Nov 21, 22, 23)
Average	-10.2	-8.9	-7.2	-7.5	-5.8	-4.6

Table 5 - Comparison of the correlation coefficient factors between the midlatitude AOH factor (MAF)/Polar ozone losses and normalized intensity of the 100hPa geopotential height wave 1 and 2 at 60° S for the years 1997-2000.

Correlation Coefficient between/for	September-October	November-December
Wave1 and MAF	0.4	-0.2
Wave 2 and MAF	0.2	0.7
Wave 1 and Polar Ozone losses	0.3	-0.2
Wave 2 and Polar Ozone losses	-0.2	0.8

Figure 1 - Schematic of zonally averaged transport in the stratosphere. The lines with arrows show the zonal-mean circulation, and the double-ended arrows indicate rapid adiabatic mixing. The shaded regions (at the edge of the polar vortex and the edge of the tropics) indicate the limits of this rapid mixing (Adapted from

<http://www.meteorology.monash.edu.au/info/techup1.pdf>).

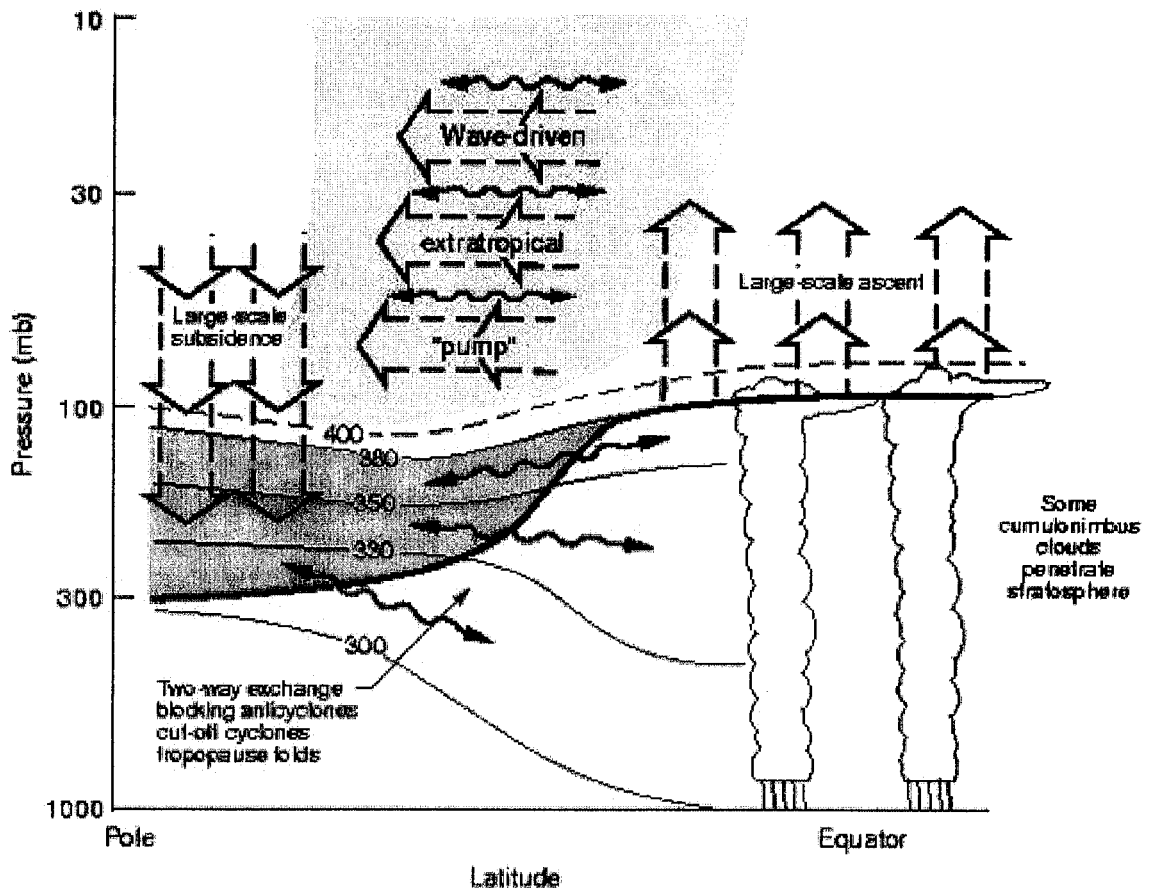


Figure 2- Annual mean, zonal mean cross section of ozone mixing ratio (ppmv) derived from MLS satellite data spanning 1991-96. Contour interval is 1 ppmv (Adapted from Atkinson 1997).

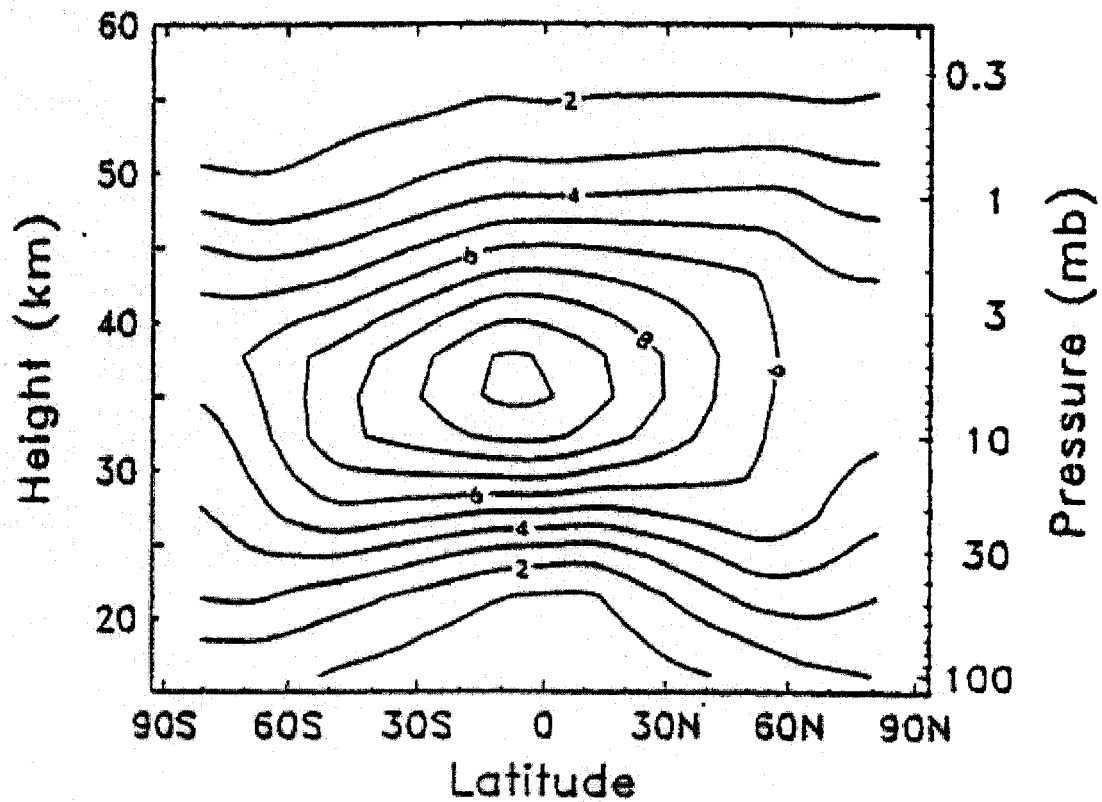


Fig. 2

Figure 3- Climatological total ozone seasonal cycle, constructed using potential vorticity coordinates (expressed in equivalent latitude). Contours are in DU. The bracketed x's denote the statistical vortex edge region in the lower stratosphere (Adapted from Randel and Wu 1995).

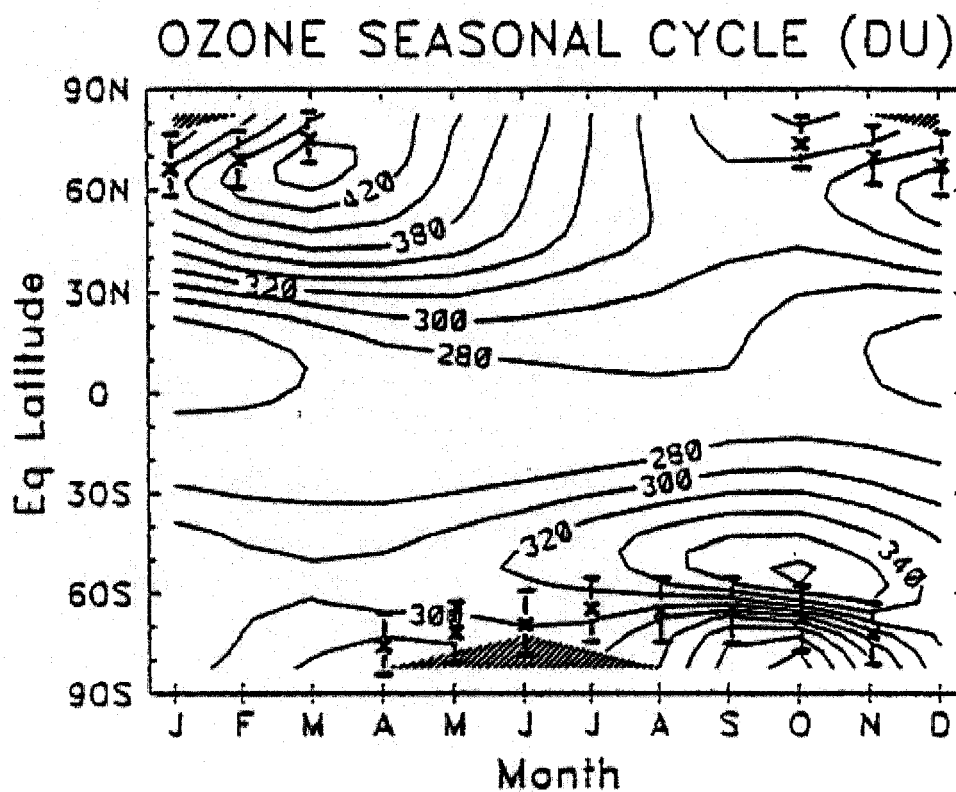


Figure 4- Daily total ozone time series from the Australian ground-based monitoring stations for the period from July 1995 to June 1996. Missing values have been replaced by the time series mean (Adapted from Atkinson 1997).

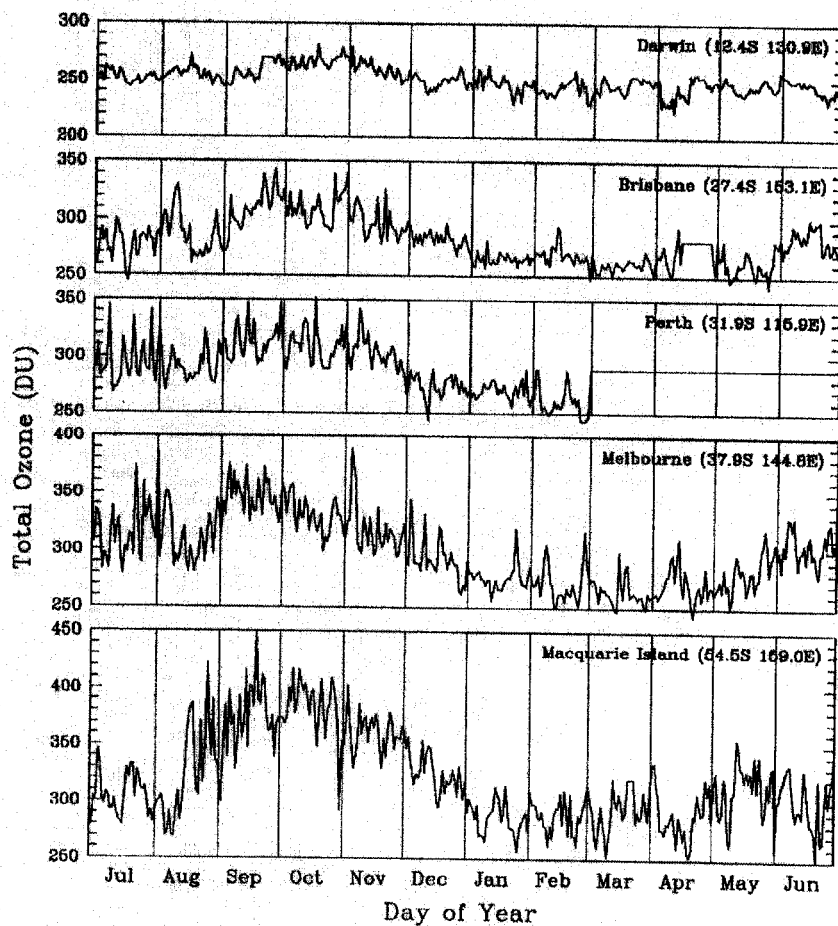


Figure 5- Measured total ozone above the Halley Bay station in Antarctica, where each point represents the average total ozone for the month of October (Adapted from http://www.atm.ch.cam.ac.uk/tour/tour_images/total_ozone.gif).

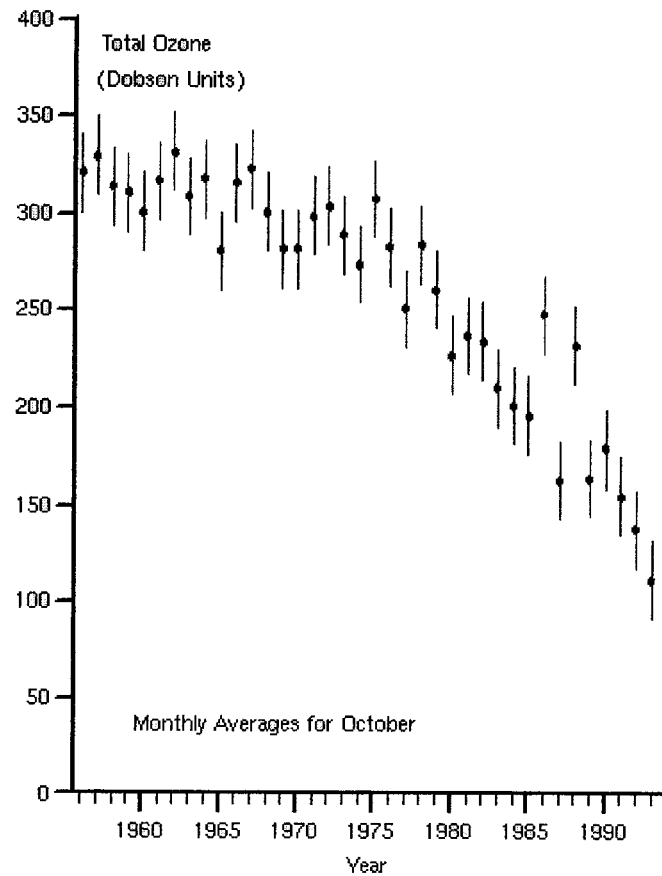


Fig. 5

Figure 6- Annual variation of Southern hemisphere polar stratospheric temperature, showing wintertime temperatures facilitating PSC type I formation that starts polar ozone losses (Adapted from NCEP-CPC Statistical and Climatological Analyses system at <http://code916.gsfc.nasa.gov>).

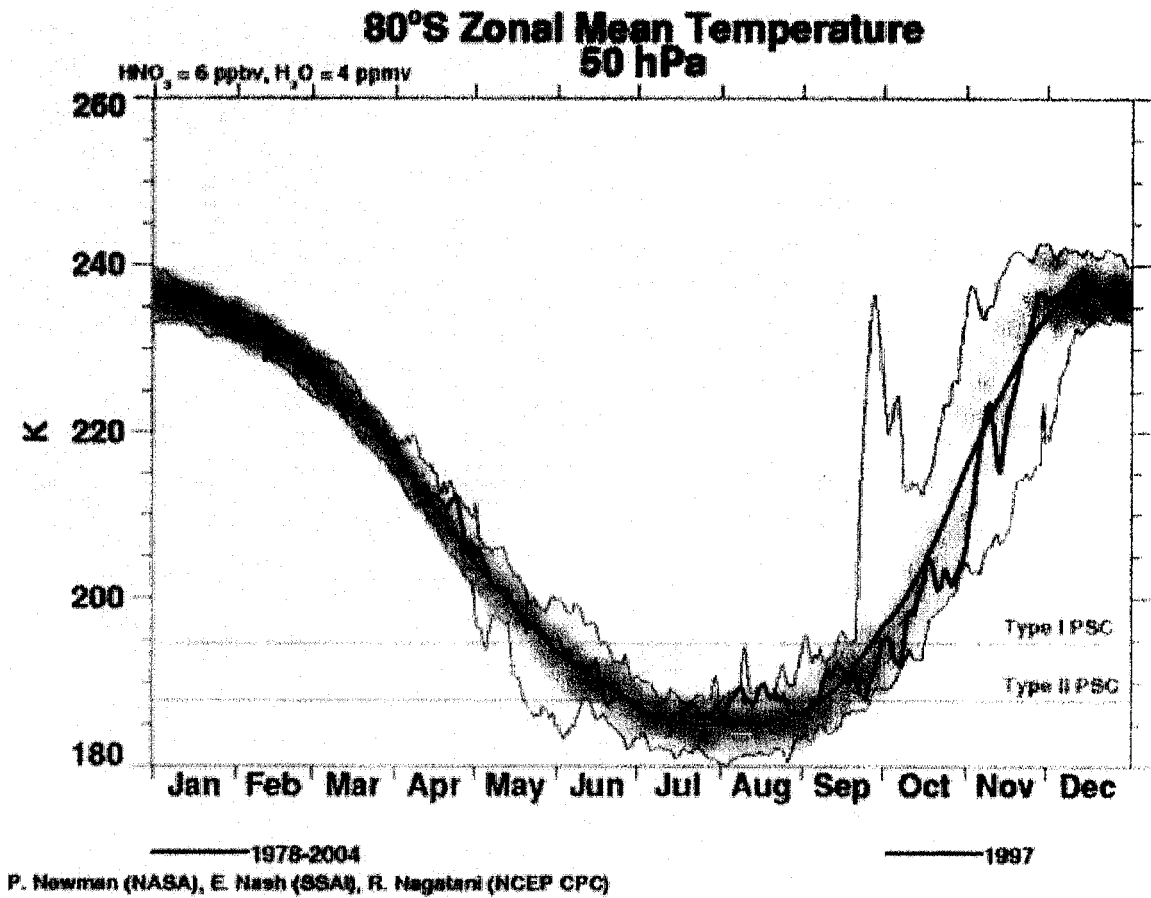


Fig. 6

Figure 7- Percentage deviations in midlatitude total ozone between 1980 and 2000 for both Northern and Southern hemispheres
(Adapted from Scientific Assessment of ozone Depletion: WMO 2002).

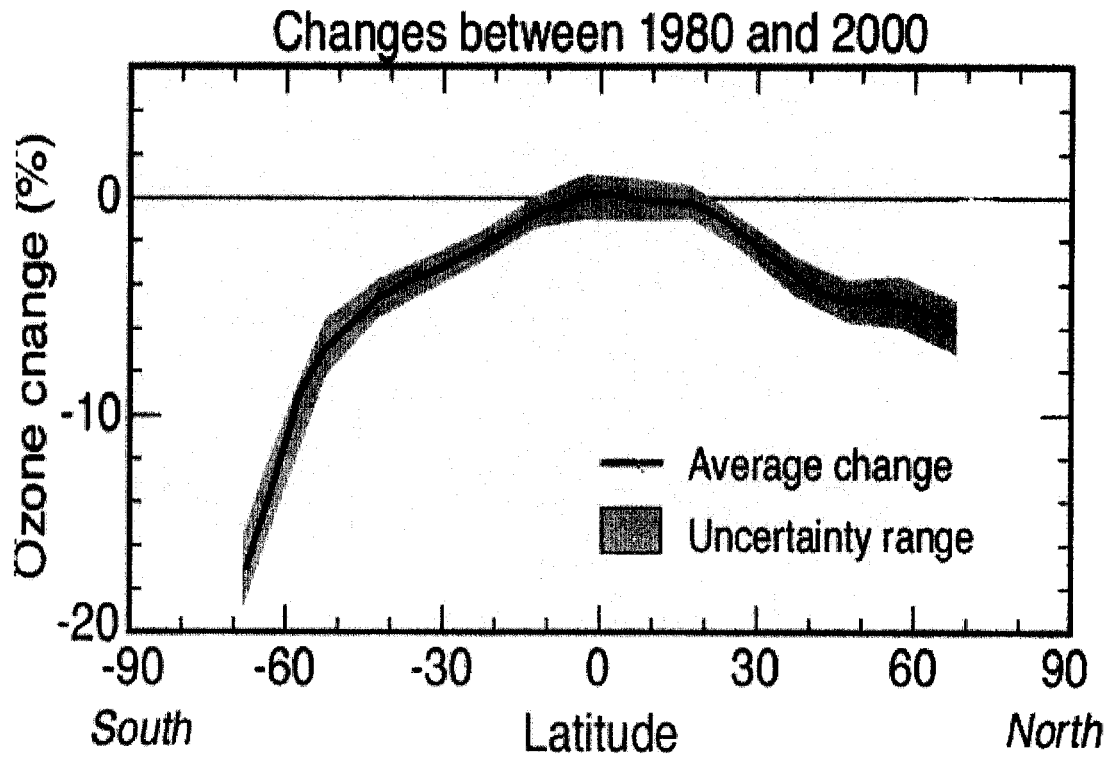
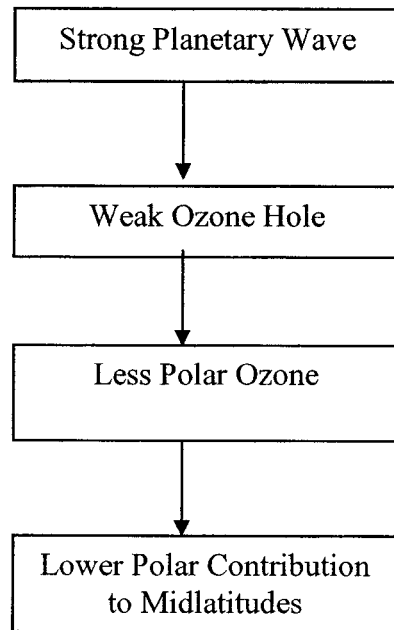


Figure 8- Schematic representation summarizing the dual roles of the extratropical planetary waves following Newman et al. 2002 and Li et al. 2002.

Newman et al. 2002



Li et al. 2002

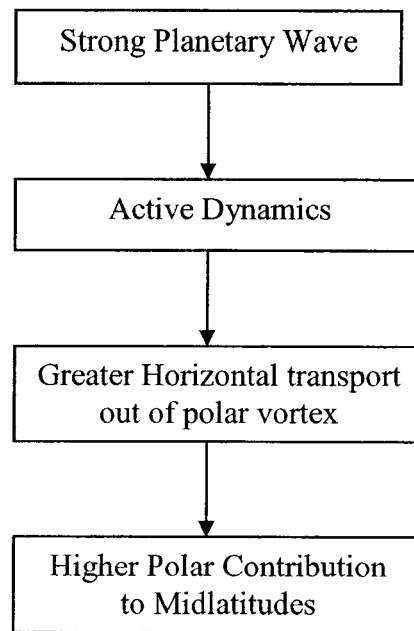


Figure 9- Total column ozone (in DU) on October 15 and November 18 of 1997 for the southern hemisphere, with left panels taken from observations (TOMS) and right panels from the CTM.

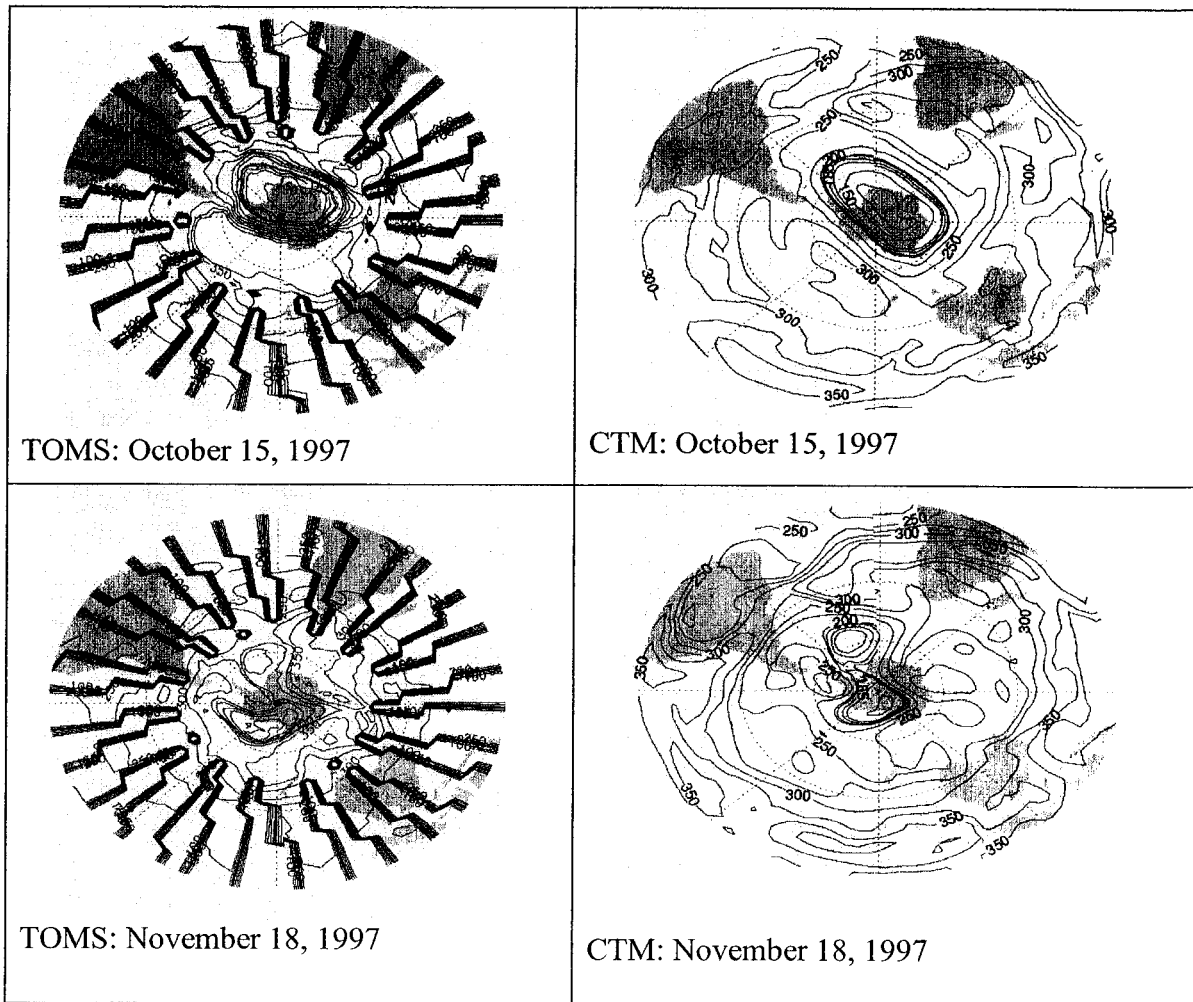


Figure 10- Vertical profile of ozone at 55°S on September 16, 1997 obtained from the CTM compared with the ozonesonde profile at the same location.

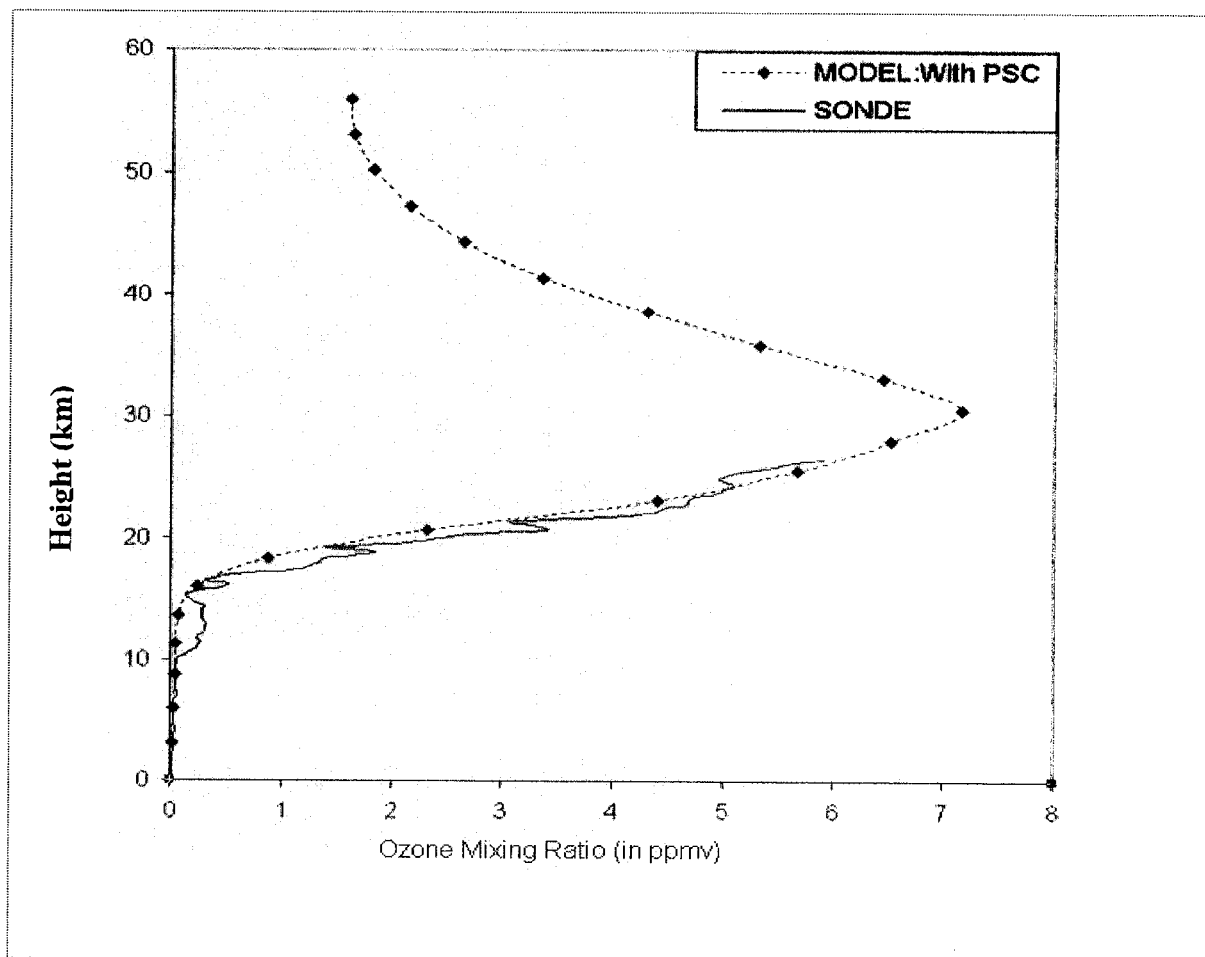


Figure 11- Production and Loss Coefficients of NASA 2-D model with and without PSC modifications at 12km on September 15.

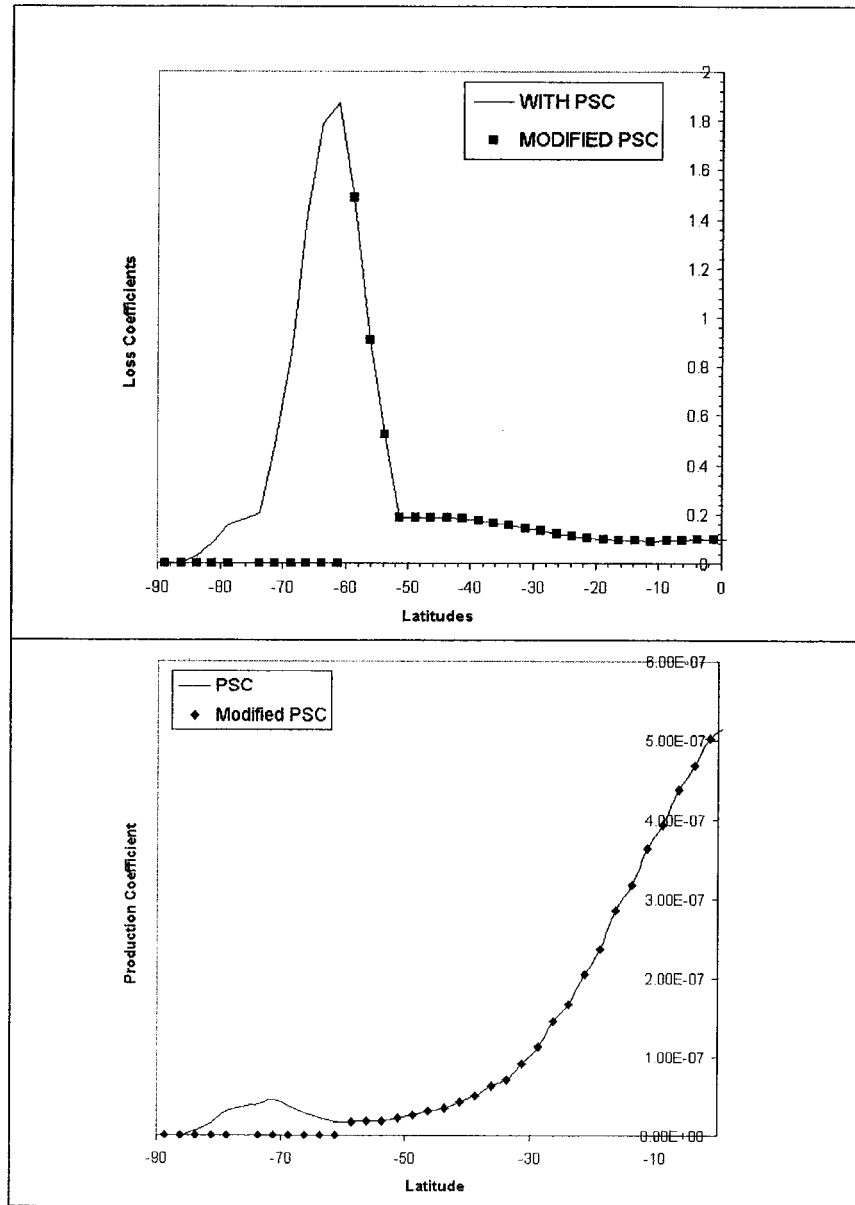


Figure 12- Difference in total ozone, in DU, between the two runs for the midlatitudes region (60°S-30°S), isolating the AOH contribution to midlatitudes, for the year 1997-2000. The plots are valid for the period September-December.

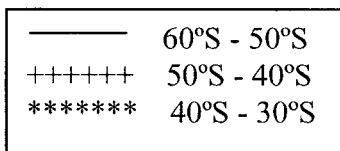
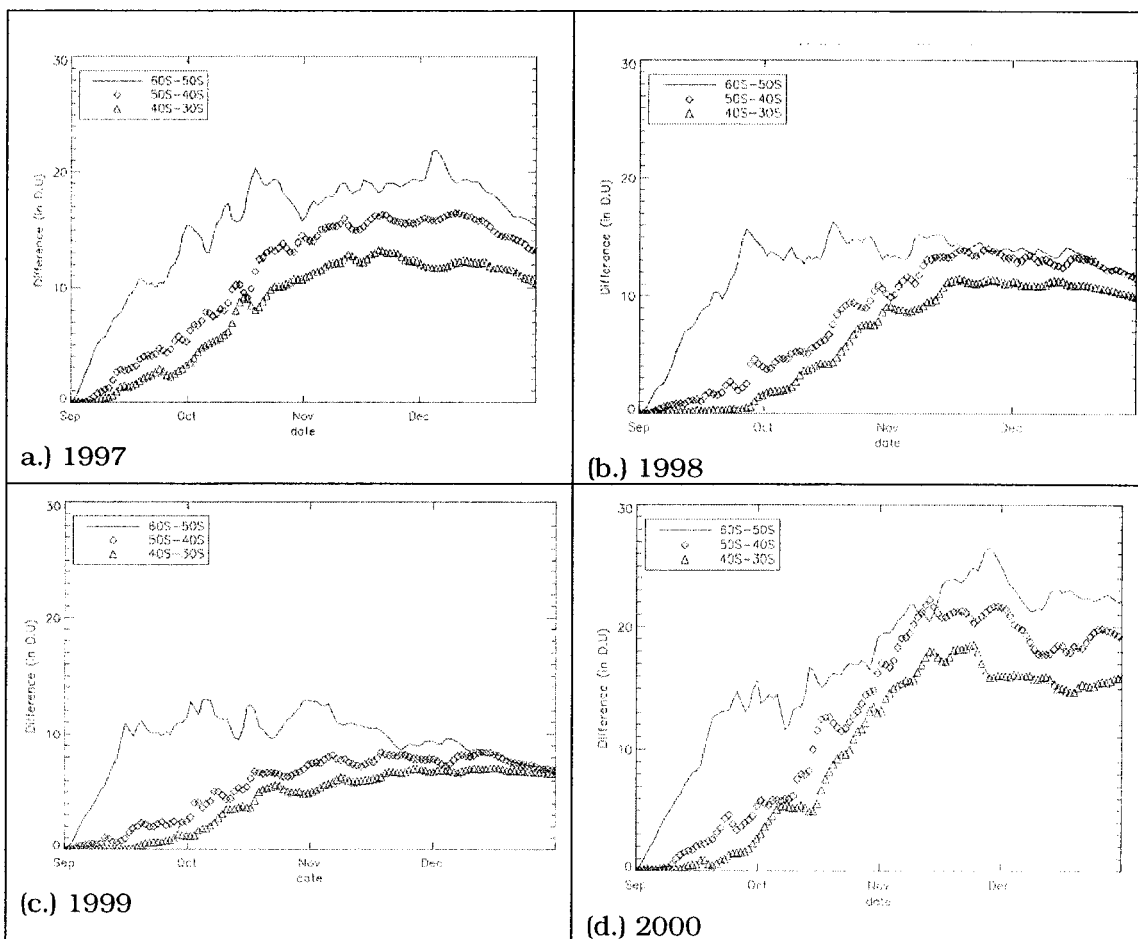


Figure 13 - Time series of the total ozone deviation in the midlatitudes (60°S-30°S) between the CTM PSC and NO PSC runs for 1997-2000.

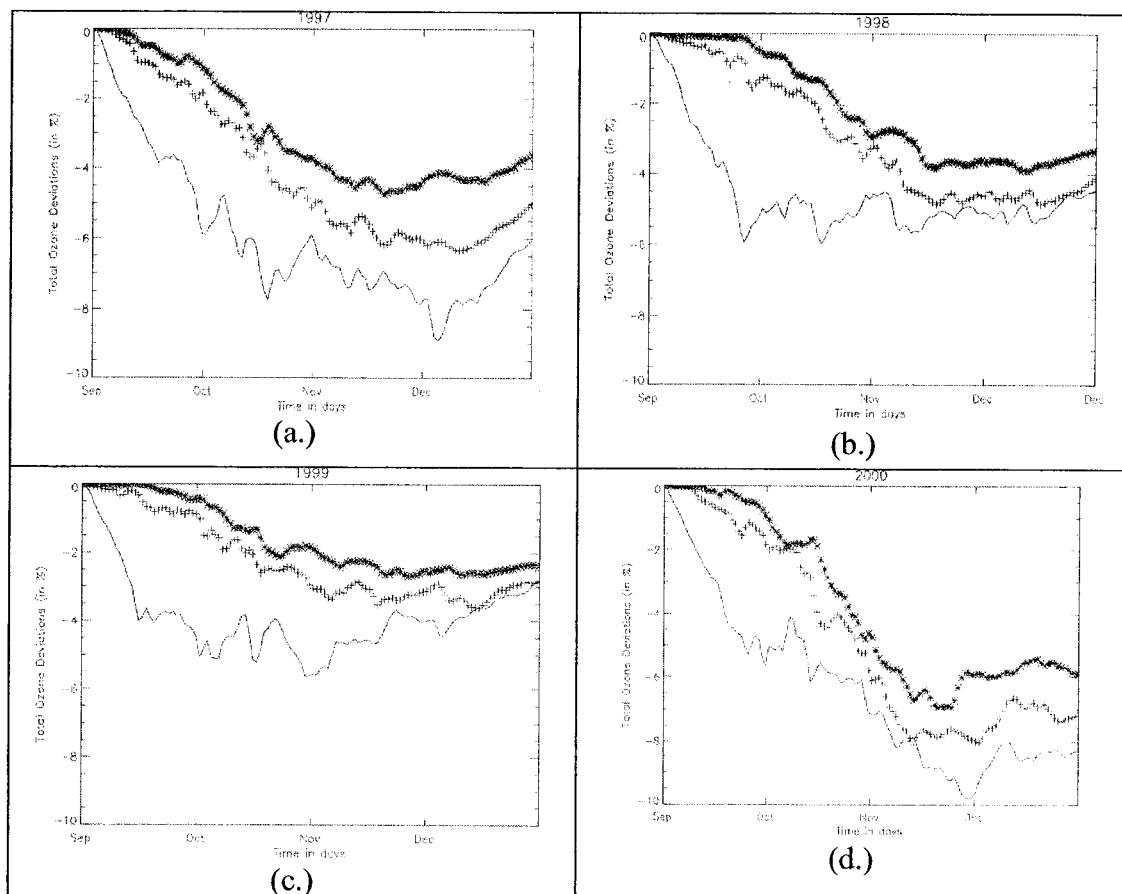


Figure 14- Total ozone at midlatitudes (60°S-30°S) from TOMS, comparing the pre-ozone hole (1979-81) with the present values (1997-99) during springtime for the September-December period.

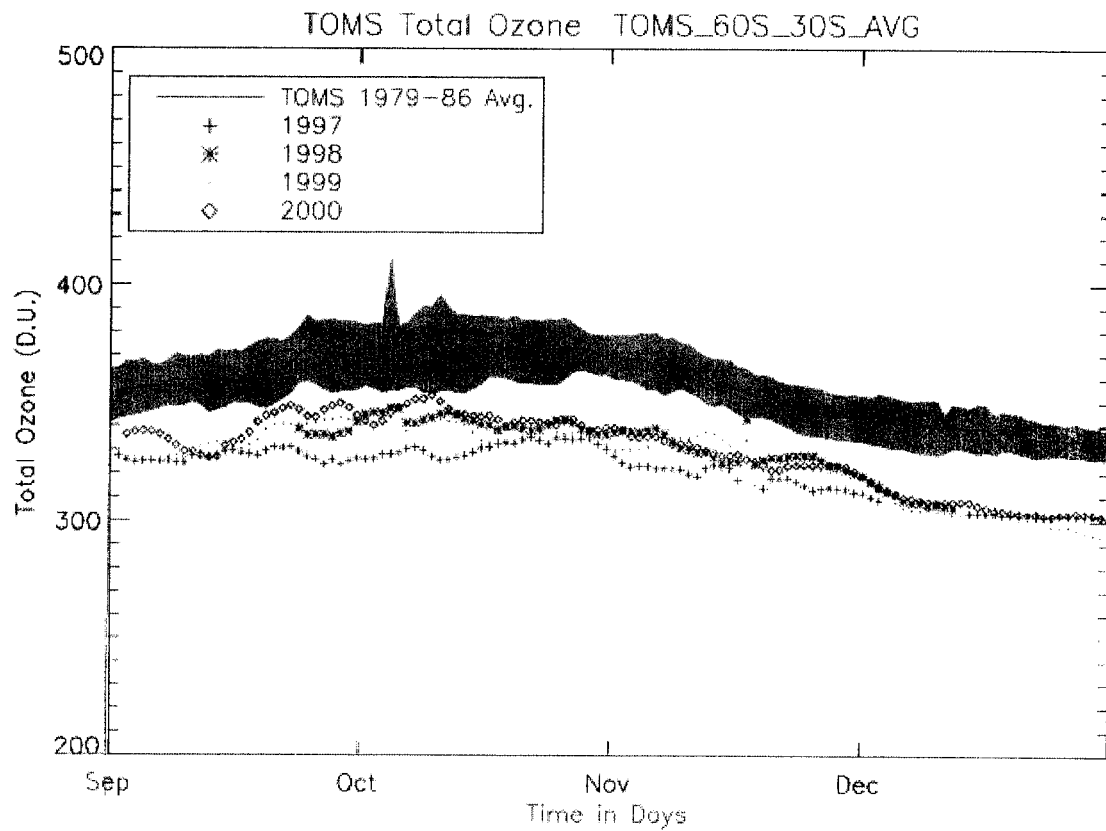


Figure 15- Interannual variation of the AOH contribution to the midlatitudes for the years 1997-2000. The plots are valid from September 1 to December 31.

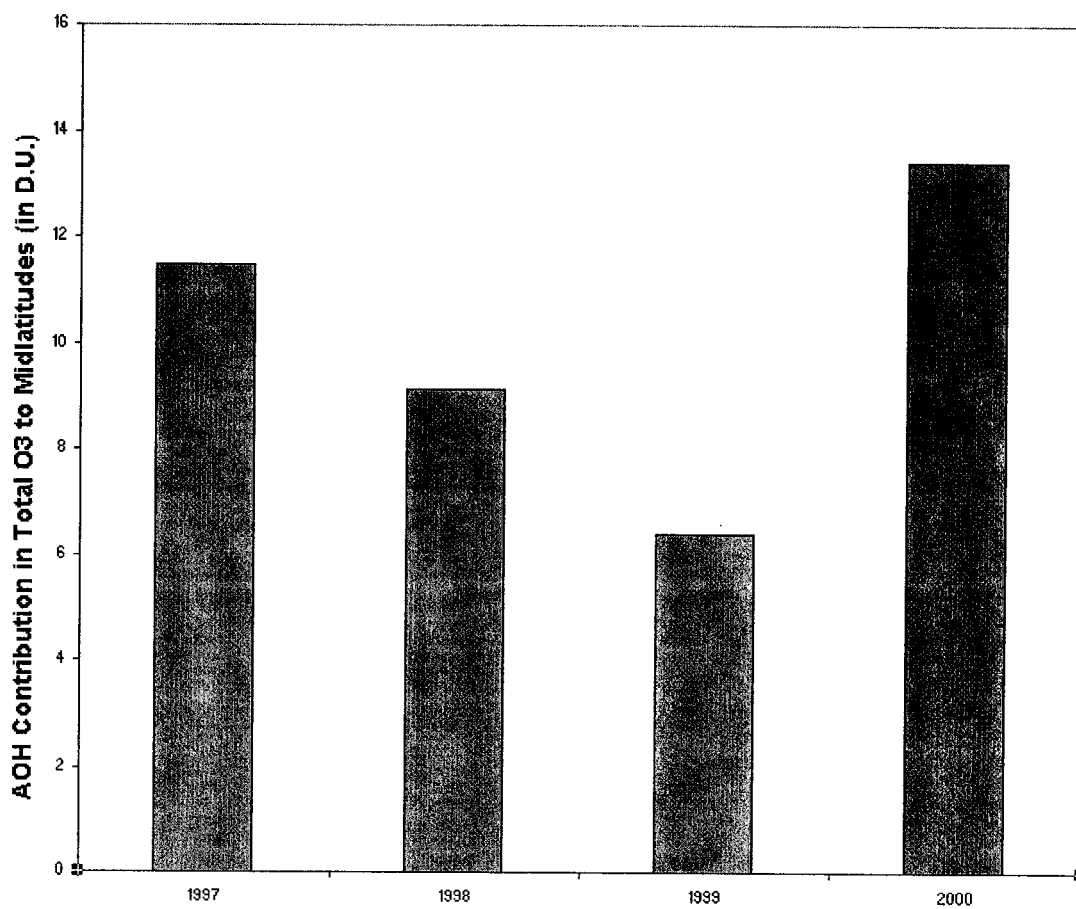


Figure 16- Scatter plots between the midlatitude region (60°S-30°S) No PSC-PSC difference in total ozone and the normalized intensity of 100hPa geopotential height wave 1 and wave 2 for the September-October period.

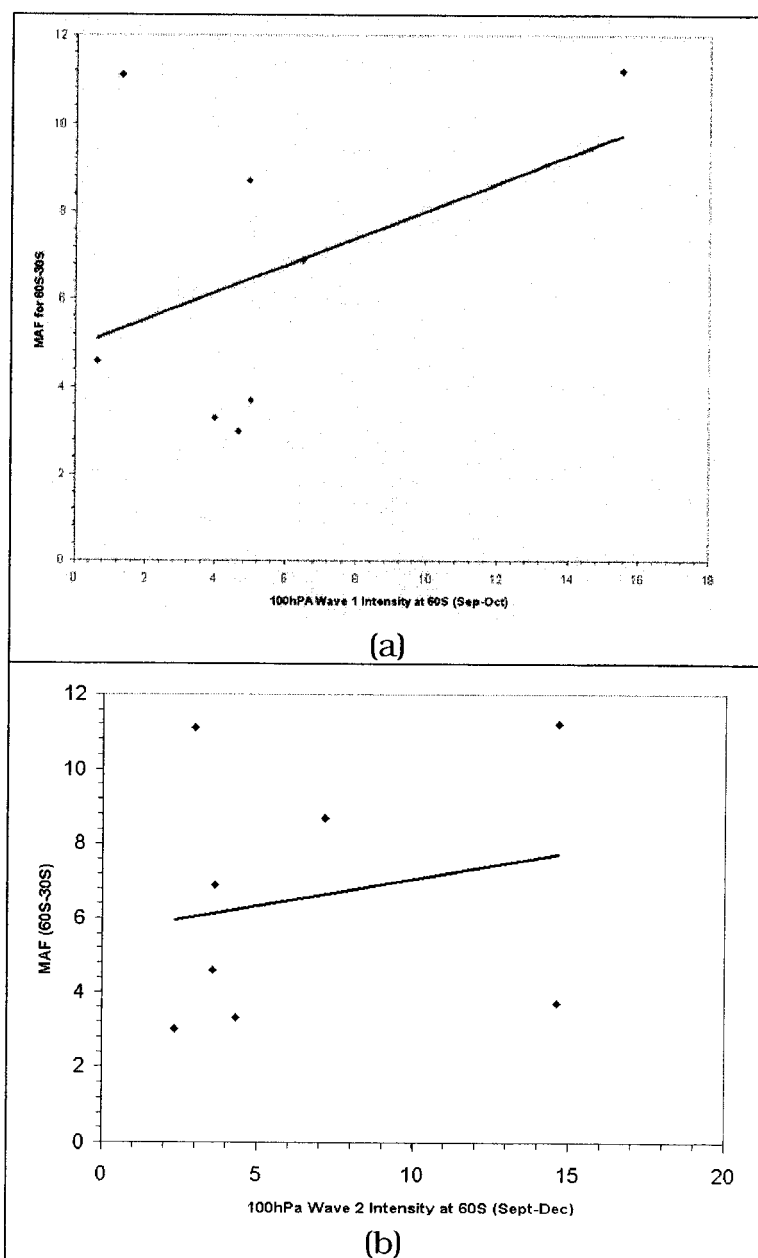


Figure 17- Same as in Fig. 16 except for the November-December period.

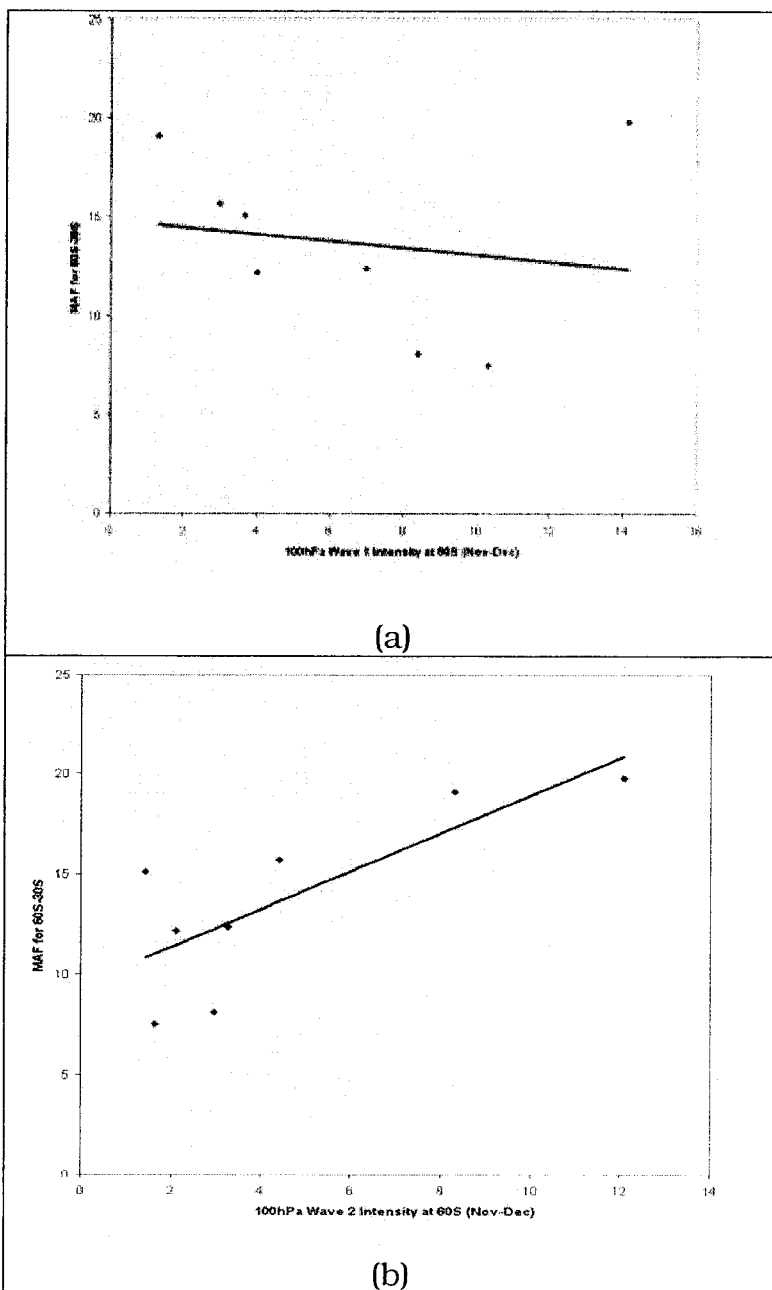


Figure 18- Comparison of the midlatitudes (60°S-30°S) No PSC-PSC difference in total ozone with the normalized intensity of 100hPa geopotential height wave 1 and wave 2 at 60° S for the 1997-2000 September–December period.

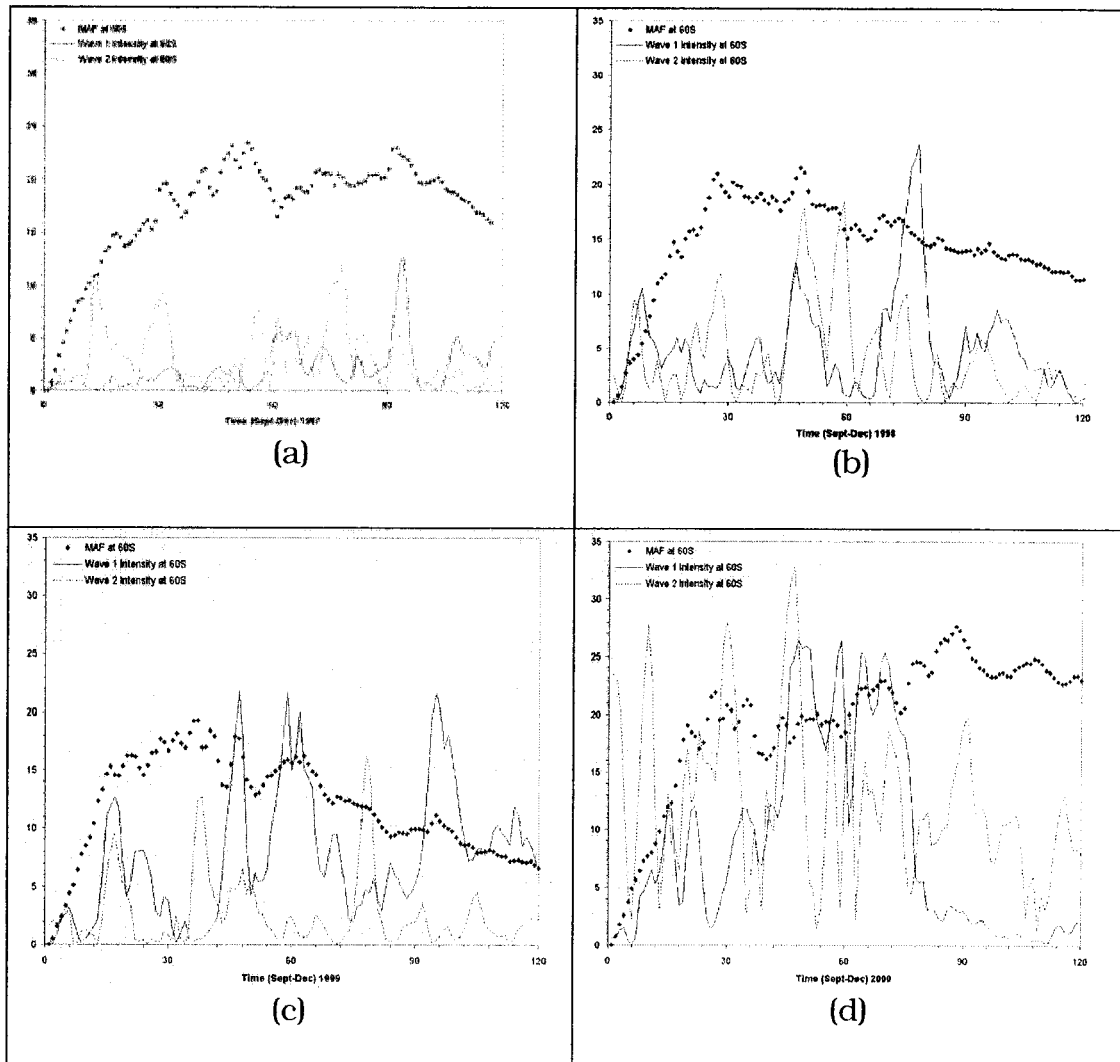


Figure 19- Scatter plots between the polar regions (90°S-60°S) No PSC-PSC difference in total ozone and the normalized intensity of 100hPa geopotential height wave 1 and wave 2 for the September-October period.

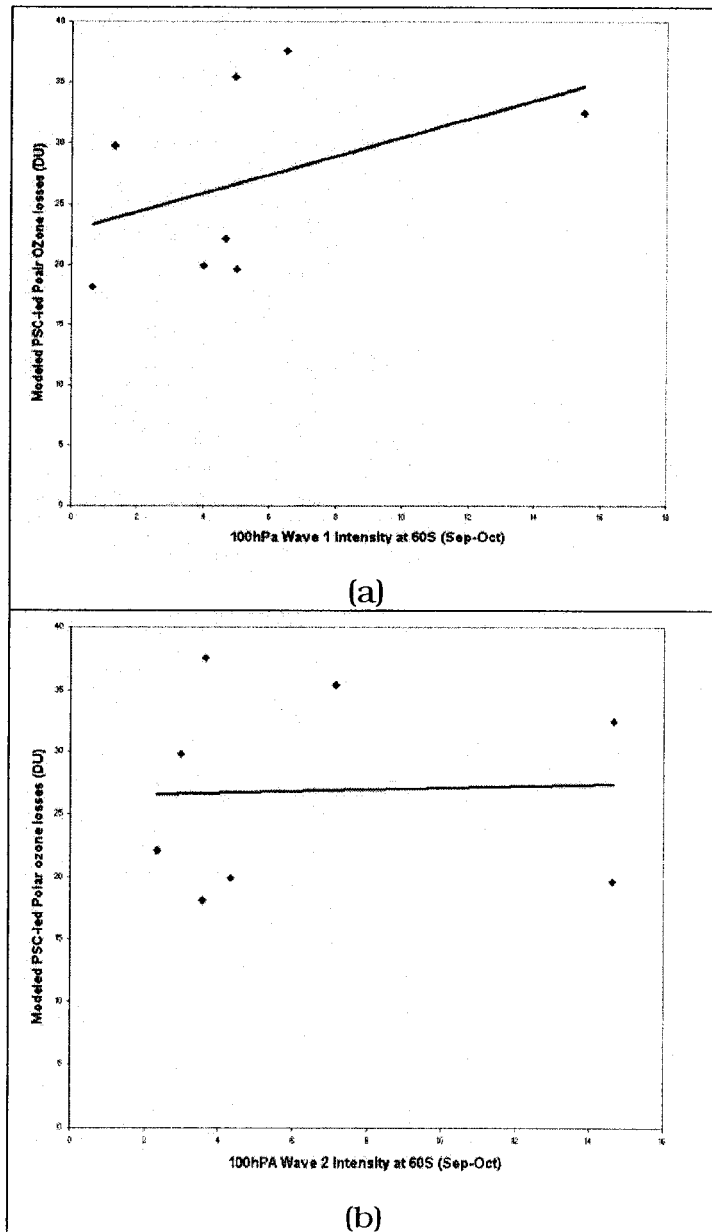


Figure 20- Same as in Fig. 19 except for the November-December period.

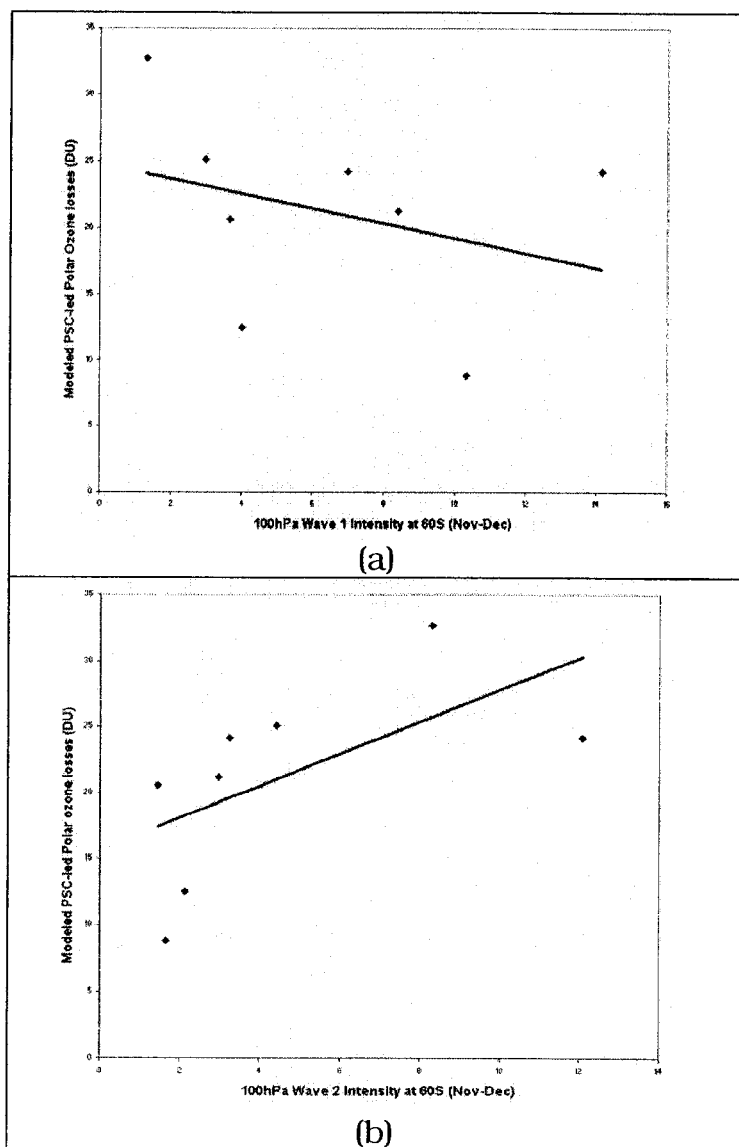


Figure 21- Comparison of the polar regions (90°S-60°S) No PSC-PSC difference in total ozone with the normalized intensity of 100hPa geopotential height wave 1 and wave 2 at 60° S for the 1997-2000 September-December period.

